A

Dissertation Report

On

Epicyclic Gear Mesh Stiffness Formulation by Displacement Method

Submitted in Fulfillment of

the Requirements for the award of Degree of

Master of Technology in Design Engineering

By

AKSHAY ARUN SHELAR

(2015PDE5198)

Under the Guidance of

Dr. T.C. GUPTA

Associate Professor

Department of Mechanical Engineering

MNIT, Jaipur

DEPARTMENT OF MECHANICAL ENGINEERING

MALAVIYA NATIONAL INSTITUTE OF TECHNOLOGY

JAIPUR –302017 (RAJASTHAN) INDIA

July-2017

DEPARTMENT OF MECHANICAL ENGINEERING
MALAVIYA NATIONAL INSTITUTE OF TECHNOLOGY

CERTIFICATE

This is to certify that the thesis entitled, "**Epicyclic Gear Mesh Stiffness Formulation by Displacement Method**" being submitted by **Shelar Akshay Arun** for the award of the degree of Master of Technology (Design Engineering) of MNIT Jaipur, is a record of bonafide research work carried out by him under my supervision and guidance. He has worked for one year on the above problem at the Department of Mechanical Engineering, Malaviya National Institute of Technology, Jaipur and this has reached the standard fulfilling the requirements and the regulation relating to the degree.

The contents of this thesis, in full or part, have not been submitted to any other university or institution for the award of any degree or diploma.

Shelar Akshay Arun
2015PDE5198

This Dissertation report is hereby approved for submission.

Date:

Dr. T.C. Gupta
Associate Professor
Department of Mechanical Engineering
MNIT, Jaipur

Place:

DEPARTMENT OF MECHANICAL ENGINEERING,
MALAVIYA NATIONAL INSTITUTE OF TECHNOLOGY,
JAIPUR-302017 (RAJASTHAN).

Candidate's Declaration

I hereby certify that the work which is being presented in the dissertation entitled "Epicyclic Gear Mesh Stiffness Formulation by Displacement Method", in partial fulfilment of the requirements for the award of the Degree of Master of Technology in Design Engineering, submitted in the Department of Mechanical Engineering, MNIT, Jaipur is an authentic record of my own work carried out for a period of one year under the supervision of Dr. T. C. Gupta, Associate Professor of Mechanical Engineering Department, MNIT, Jaipur. I have not submitted the matter embodied in this dissertation for the award of any other degree.

Place: Jaipur
Date: 07 July, 2017

Shelar Akshay Arun
M. Tech (D.E.)
ID: 2015PDE5198

Acknowledgement

First, to my parents, for their support and providing strength throughout my life and for instilling in me at an early age the value as well as importance of education.

I am deeply grateful to my mentor **Dr. T.C. Gupta** for his constant encouragement and instruction and insight throughout this endeavor. His moral support and valuable feedback have been a great source of inspiration for enhancing my work in this dissertation work.

I am extremely grateful to respected **Dr. Himanshu Chaudhary, Dr. Dinesh Kumar** and **Dr. Amit Singh** for being supportive and helpful.

Lastly, I would like to thank **Manoj Gupta**, **Harsh Dixit** and **Ajit Singh** (Ph.D. Research Scholar) for helping me throughout my dissertation work.

Shelar Akshay Arun
Design Engineering
(2015PDE5198)

Abstract

This thesis contains the formulation of a geared system dynamic model for an epicyclic gear train. The two dimensional spur gear model is developed using one orientation angle. A 6X6 mesh stiffness matrix is derived for each meshing pair like sun gear-planet gear, ring-planet gear and carrier-planet gear. Its effect is considered in the vibration of the whole geared system. Natural frequencies are determined and compared with the Matlab results. Hence, using the formulation of this paper, the robust rotor dynamic model for an epicyclic geared system is developed. Mode shapes and some important graphs are plotted.

Table of Contents

1 Introduction 1

1.1 Introduction 1

1.1 Thesis Outline 3

2 Literature Review, Scope and Objective 4

2.1 Literature Review 4

2.2 Research Objective 5

3 Methodology for Calculating Gear Mesh Stiffness 6

3.1 Gear Mesh Stiffness Calculation for Spur Gear 6

3.1.1 Methodology 6

3.1.2 Modeling of Spur Gear Using Inventor Professional 2016 9

3.1.3 Various Boundary Conditions, Applied Loads and Displacements 11

3.1.4 Results and Comparison 13

3.1.4.1 Ring-planet mesh 13

3.1.4.2 Sun-planet mesh 14

3.1.4.3 Comparison 14

4 Gear-Mesh Model Methodology with Application 16

4.1 Gear Mesh Model Methodology 16

4.1.1 Development of Gear Mesh Forcing Function 16

4.1.2 Geometry and Loading Conditions 17

4.1.3 Gear-Mesh Coordinates System 19

4.1.4 Force and Moment Equations 20

4.1.5 Displacement Method 21

4.1.5.1 Sun-Planet Mesh (Forces on the sun gear) 21

4.1.5.2 Ring-Planet Mesh (Forces on the ring gear) 23

4.1.5.3 Carrier-Planet Mesh (Forces on the carrier) 24

4.1.5.3.1 Vertical Force Acting on the Carrier 24

4.1.5.3.2 Horizontal Force Acting on the Carrier 25
4.1.5.4 Sun-Planet Mesh (Forces on the planet gear) 27
4.1.5.5 Ring-Planet Mesh (Forces on the planet gear) 28
4.1.5.6 Carrier-Planet Mesh (Forces on the planet gear) 29
4.1.5.6.1 Vertical Force Acting on the Planet 29
4.1.5.6.2 Horizontal Force Acting on the Planet 30
4.1.6 Influence Coeffiecient Method 31
4.1.7 Finding out the meshing frequency 31
4.2 Application 32
4.2.1 System and System Parameter 32
4.2.2 Results of Meshing Epicyclic Gears 32
4.2.3 Validation 33
5 Results 35
5.1 Mode Shapes 35
5.2 Sensitivity of Natural Frequency 42
5.2.1 Sensitivity due to Change in the Sun Gear Mass 42
5.2.2 Sensitivity due to Change in the Ring Gear Mass 43
5.2.3 Sensitivity due to Change in the Planet Gear Mass 43
43
6 Conclusions and Recommendations 45
6.1 Conclusions 45
6.2 Limitation 45
6.3 Recommendations 46
References 47
Appendix A: Finite Element Matrix Equations 48
A.1 48

List of Figures

Figure 3.1: Coupling between the transverse and torsional motions of the gear 6
Figure 3.2: Meshing gears 7
Figure 3.3: CAD model: Epicyclic Gear Set 10
Figure 3.4: Boundary conditions and applied load (input torque) for the analysis 11
Figure 3.5: Boundary conditions in ANSYS Workbench 15.0 for ring-planet mesh 11
Figure 3.6: Displacement field in ANSYS Workbench 15.0 for ring-planet mesh 12
Figure 3.7: Boundary conditions in ANSYS Workbench 15.0 for sun-planet mesh 12
Figure 3.8: Displacement field in ANSYS Workbench 15.0 for sun-planet mesh 13
Figure 4.1: Finite element representation of a Gear Pair 16
Figure 4.2: Epicyclic Gear Model 17
Figure 4.3: Forces acting on the spur gear 18
Figure 4.4 Force Components 18
Figure 4.5: Relation between Local and Global Axes 19
Figure 4.6: Contribution of displacements to the Line-of-Action (sun-planet mesh) 21
Figure 4.7: Contribution of the rotational motion about z_i in the movment of the pitch point 21
Figure 4.8: Contribution of displacements to the Line-of-Action (ring-planet mesh) 23
Figure 4.9: Contribution of vertical force to pitch point movement (carrier-planet mesh) 24
Figure 4.10: Contribution of horizontal force to pitch pt movement (carrier-planet mesh) 25
Figure 4.11: Force on the planet gear due to sun-planet mesh 27
Figure 4.12: Force on the planet gear due to ring-planet mesh 28
Figure 4.13: Vertical force on the planet gear due to carrier 29
Figure 4.14: Horizontal force on the planet gear due to carrier 30
Figure 5.1: Rotational Mode 35
Figure 5.2: Translational Mode 37
Figure 5.3: Radial Planet Mode 39
Figure 5.4: Translational Planet Mode 39
Figure 5.5: Rotational Planet Mode 40
Figure 5.6: ω (rad/s) vs. ms (kg) Plot 42
Figure 5.7: ω (rad/s) vs. mr (kg) Plot 43
Figure 5.6: ω (rad/s) vs. mp (kg) Plot 43

List of Tables

1	Table 3.1: Parameters used to create epicyclic gear in Inventor professional 2016	10
2	Table 4.1: System Parameters	33
3	Table 4.2: Natural Frequencies (Hz) of Meshing Epicyclic Gears	33
4	Table 4.3: Comparison of Natural Frequencies	34
5	Table 5.1: Rotational mode natural frequencies	35
6	Table 5.2: Rotational Mode Shapes (Matlab)	36
7	Table 5.3: Translational Mode Natural Frequencies	37
8	Table 5.4: Translational Mode Shapes (Matlab)	38
9	Table 5.5: Planet Mode Natural Frequencies	40
10	Table 5.6: Planet Mode Shapes (Matlab)	41

Nomenclature

LOA	Line of Action
E	Young's modulus
$[K]_{mesh}$	Gear mesh-stiffness matrix
$[K_{ii}]$	Sub matrix of Gear-mesh stiffness matrix
$\{q\}$	Displacement vector
$\{F\}$	Force vector
F_n	Normal force along LOA
ht	Gear height
r_{1b} , r_{2b}	Base circle radius of gear 1 and 2 respectively
r_{1p} , r_{2p}	Pitch radius of pinion and gear respectively
θ_1 , θ_2	Angular displacement of gear 1 and 2 respectively
b	Tooth width
C.R.	Contact Ratio
N_1, N_2	Number of teeth of gear 1 and 2 respectively
K_{hx}, K_{hy}	Translational bearing stiffness of the components
K_m	Linear tooth mesh-stiffness
K_{hu}	Rotational bearing stiffness of the components
K_t	Torsional gear-mesh stiffness
K_{hn}	Meshing stiffness between other components and planet
K_p	Planet bearing stiffness
T_{in}, T_1	Input torque
X,Y and Z	Global coordinates
X',Y' and Z'	Prime coordinates
ξ, η	Radial and tangential coordinates
$\phi_x, \phi_y,$ and ϕ_z	Direction cosine
S	Arc length of base circle of gear
φ	Orientation angle in helical gear
i, j	Node i and j

ω	Natural Frequency
m	Multiplicity

1 Introduction

This chapter contains the introduction to planetary (epicyclic) geared system.

1.1 Introduction

Gear drive is a positive drive which is used to transmit the power, provided when the two shafts are at the short distance. It is used in many power transmission systems like a helicopter, in automobile to transmit the power from engine to wheels, watches, some power generating devices like turbines, aircrafts, in other industrial systems and many household appliances.

A critical failure of the rotor system can result in the massive damage to the system and in some cases, may result in the loss of life. So, for the sake of maintenance and reliability it is needed to predict resonating frequency of these systems. In many of these systems, various components like gear box can cause some difficulties in calculation and prediction of these resonating frequencies. Different gearboxes have different configurations and various complex configurations.

Since the starting period of rotational systems, gear has been a must part of it. However, many characteristics of the gearbox still need the better conception. In the geared rotor system, usage of gears can generate as well as transmit vibrations throughout the given system. Various factors like the excitation forces produced due to some unbalance or misalignments can change the stiffness properties.

The study of gear dynamics in the systematic and scientific way started in the late 1920s. Basic objectives of the gear dynamics are extensive. It includes various phenomena like pitting, scoring, corrosive wear, bending stress, reliability, gyroscopic effect and expected gear life. Gear dynamic model as the spring-mass system got emerged in late 1950s. It took 1970s for the first finite element model. Formulation of a geared system as a spring mass system brought it closer in the continuum system formation.

Basically, epicyclic gear system is a set of gears in which a gear called as a planet rotates around the centrally mounted gear called the sun gear. There can be as many numbers of the planets as per the application. Carrier is used to connect the centers of these two gears. Epicyclic geared system can be assembled so that the planet rolls inside the outer gear called as the ring gear. The epicyclic train in which the planet gear meshes with the central gear ‘sun’ as well as the outer gear ‘ring’ is known as ‘Planetary Gear Train’.

While epicyclic gears consist of planets which are turned around by the rotating carrier, they can also use the outer gear 'ring' which meshes with the planets. Planetary gears can be divided as simple planets and compound planets. Simple planetary system has one central sun gear, one carrier, one outer ring gear and a set of planets. On the other hand, compound planetary system has been categorized as:

- Meshed planets system- Consists of two or more planets in the mesh.
- Multi stage system- The system consists of two or more planets.
- Stepped planet system- Planets are connected by shafts in each planet train.

All the gears are usually coaxial but in some cases, shafts can be inclined with each other. In the epicyclic system consisting two planets meshing with each other, one planet meshes with the sun while the other one with the ring. In a particular case, if the carrier is fixed, sun and the outer ring gear rotate in the same direction and give the reverse output when compared with the standard epicyclic geared system.

Epicyclic gears can have various arrangements in which the input as well as output members can be changed.

- Less speed more torque- In this configuration, the input is given to the sun gear, while the carrier is kept stationary and output is obtained from the ring.
- More speed less torque (Same Direction) - In this configuration, Carrier is the driving member, while the ring is kept stationary and the driven member is the sun gear.
- More speed less torque (Reverse Direction) - In this configuration, Ring gear is the driving member, carrier is kept stationary while the sun gear is the driven member.

These gears are basically used in the aircraft engines, choppers and marine vehicles. Epicyclic gears dominates parallel gears in many fields like compactness, transmission of higher torques, distributed load on planets and thus very small loads on the shaft bearings as well as reduced vibrations and lower noise level due to relatively smaller system components.

This work includes the finite element model with 6 degrees of freedom per element. Mesh stiffness matrix with the order 6x6 has been formed for each meshing pair i.e. sun-planet, planet-ring and carrier-planet. Mesh stiffness value is determined using the analysis software for the epicyclic geared system. Equations are developed for various mesh stiffness components. Thereafter natural frequencies of the given system are determined and matched with the research paper.

1.1 Thesis Outline

1. Chapter 1 contain basic introduction about the gear dynamics.
2. Chaper 2 contain a comprehensive literature review on the epicyclic gear dynamics and discuss scope and objective of the work.
3. Chapter 3 contain a method to find non-linearity of the gear-mesh stiffness during the one mesh cycle. By using FEA software average gear mesh stiffness for the epicyclic gear can be found.
4. Chapter 4 provides a detailed discussion of development of 6 DOF gear mesh stiffness.
5. Chapter 5 contains some important results like mode shapes and sensitivity of natural frequencies.
6. Chapter 6 provides conclusion, limitation and recommendation of gear-mesh model of spur helical gear.

2 Literature Review, Scope and Objective

2.1 Literature Review

A detailed dynamic analysis of epicyclic gears started in the early 1980s, (August 1983). Gear dynamics including free vibration investigation and vibration analysis was done, (Cunliffe et al., 1974; Botman, 1976). Cunliffe used thirteen degree of freedom system and found out the natural frequencies as well as vibration modes. More analytical work was performed after 1990s. A time-varying and nonlinear model was developed by Kahraman (1994a) and extended to the three dimensional model. Kahraman also investigated mesh phasing and load sharing between the planetary gears. This formulation permits the analysis of the planet meshing with the carrier, ring or sun with any numbers of the planetary gears which are placed at the arbitrary positions.

In some analyses (Botman 1976, Kahraman 1994), gyroscopic effects on the proposed lumped parameter models have not been considered. It was found that these effects can cause much difference when the system works at the higher speeds. Free vibration analysis is a critical analysis which calculates some important factors such as system natural frequencies and vibration mode shapes. Botman (1976), Frater et al. (1983), Kahraman (1994) have done work this field.

Kahraman (1994) formulated a system with 6X6 mesh stiffness matrices for the given gear mesh. While Botman (1976) formulated spur planetary gear system having eighteen degrees of freedom. All these vibration modes can be categorized into translational, rotational and planet modes. Effects of planet bearing stiffness as well as rotation of carrier on the natural frequencies were studied numerically.

Frater et al. (1983) extended Botman's work about natural frequencies by considering the unequal planet mesh stiffness. David Blake Stringer (2008) presents methodologies for rotor dynamic modeling of rotary-wing transmission based on the first principle. He developed three-dimensional finite element model of gear mesh stiffness for spur and helical gears. Another finite element formulation to determine the coupled vibration characteristic of a geared rotor system is proposed by Rao(1995). His work on sensitivity analysis of various parameter on system natural frequencies and mode shape such as pressure angle etc.

S.B. Wadkar (2005) examined the effect of various parameters on the variation of the gear mesh stiffness. He proposed a method to find mesh stiffness from the combined torsional mesh stiffness of the gear pair.He explains how is the mesh stiffness of the gear pair increases when the second pair of gear tooth are in contact.

While calculating the natural frequency, mesh stiffness variations can become complicated due to many factors such as transmission error excitation (Smith, 1983) as well as contact loss non-linearity (Blankenship and Kahraman, 1995). Time varying mesh stiffness value can be calculated using the formulation by Fourier's series. While in most of the cases, it is safe to assume that there is no teeth contact loss as it takes place for the quite smallest time period.

2.2 Research Objective

This study primarily focus on the non-linear mesh stiffness of different gear pairs in the epicyclic gear set like sun-planet, planet-ring and planet-carrier affecting the overall stiffness and hence the vibrational characteristics of the system. The gear mesh stiffness effect is taken into account using 6X6 gear mesh stiffness matrix for each meshing pair. To conduct all this analysis, Matlab codes are to be developed to determine the natural frequencies of the system.

3 Methodology for Calculating Gear Mesh Stiffness

This chapter contains a calculation of the gear mesh stiffness for the spur gear using the methodology provided and softwares such as ANSYS Workbench 15.0 and Inventor Professional 2016. The equations provided for mesh stiffness calculation are then modified for each meshing pair in the epicyclic gear set.

3.1 Gear Mesh Stiffness Calculation for Spur Gear

3.1.1 Methodology

Torsional stiffness and linear tooth mesh stiffness are related. The gear mesh stiffness can be easily understood by the torsional and transverse motion of the gear system. Figure 3.1 shows relation between transverse and torsional motion.

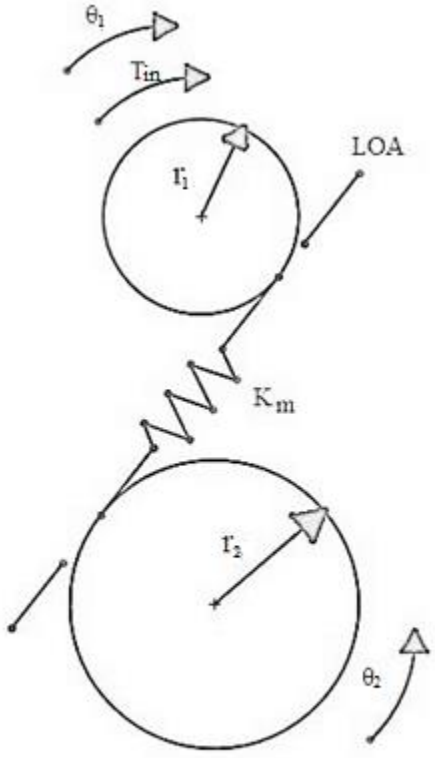

Figure 3.1: Coupling between the transverse and torsional motions of the gear

Where,

T_{in}= Torque input (Nm)

r_1 = Base circle radius of gear 1 (m)

θ_1= Angular displacement of gear 1 (rad)

r_2= Base circle radius of gear 2 (m)

θ_2= Angular displacement of gear 2 (rad)

K_m= Linear tooth mesh stiffness (N/m)

LOA= Line of action

When the gear pair meshes, torsional meshing stiffness is the important factor. It is assume that, during the meshing, pitch circle of the first gear rolls on the other one without slipping.

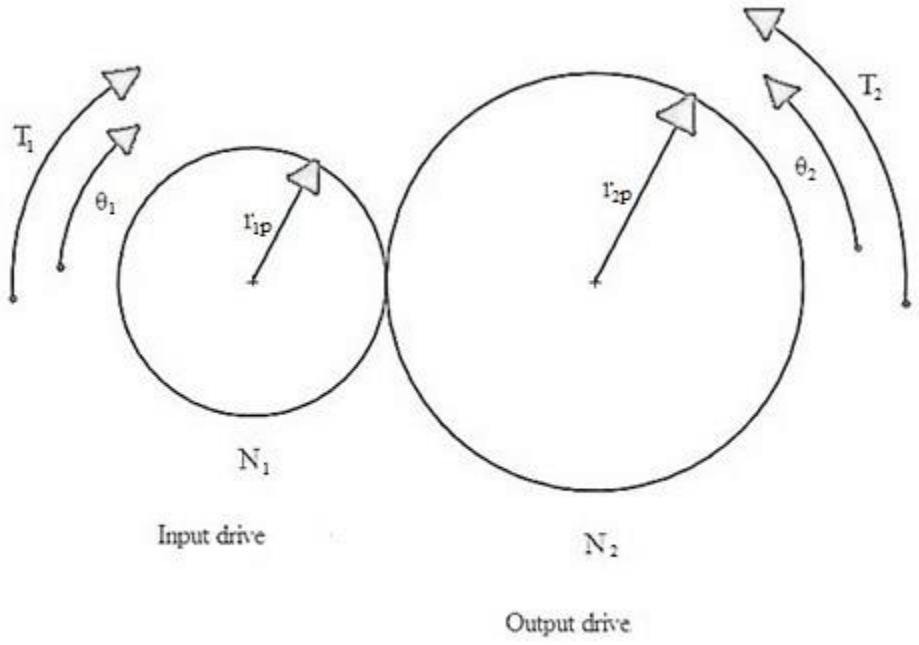

Figure 3.2: Meshing gears

Where,

T_1 = Input torque (Nm)

θ_1 = Angular displacement of gear 1 (rad)

r_{1p} = Pitch radius of gear 1 (m)

N_1 = Number of teeth of gear 1

T_2 = Output gear torque (Nm)

θ_2 = Angular displacement of gear 2 (rad)

r_{2p} = Pitch radius of gear 2 (m)

N_2 = Number of teeth of gear 2

The length of displaced arc will remain same for the meshing gears, which gives the following equation,

$$r_1 \theta_1 = r_2 \theta_2 \tag{3.1}$$

$$\frac{N_1}{N_2} = \frac{r_1}{r_2} = \frac{\theta_2}{\theta_1} \tag{3.2}$$

Assuming that there is no power loss,

$$T_1\theta_1 = T_2\theta_2 \tag{3.3}$$

$$\frac{N_1}{N_2} = \frac{T_1}{T_2} = \frac{\theta_2}{\theta_1} \tag{3.4}$$

Torsional mesh stiffness can be given as the ratio of the applied torque and the angular deflection of the same.

$$K_t = \frac{T}{\theta} = \frac{T_2}{\theta_2} = \frac{T_1}{\theta_1} \tag{3.5}$$

Where,

T = Applied torque (N/m)

θ = Angular deflection (rad)

K_t = Torsional mesh stiffness (Nm/rad)

The linear tooth mesh stiffness is given by the ratio of force along the 'Line of Action' (F_n) and the linear deflection of gear along a base circle (S).

$$K_m = \frac{F_n}{S} \tag{3.6}$$

K_m = linear tooth mesh stiffness (N/m)

F_n = Normal force along the line of action (N)

S = Arc length of the base circle of gear (m)

Mathematically, torque is given by the cross product of the force vector and the position vector , which in the case here is base circle radius r_1. Thus, $T = F_n \times r_{1b}$. Furthermore, assuming θ is very small, $\theta = S / r_{1b}$. S is an arc length of the base circle of the gear 1. Hence, linear tooth mesh stiffness is given as,

$$K_m = \frac{F_n}{s} = \frac{\frac{T}{r_{1b}}}{r_{1b} * \theta} = \frac{T}{\theta * {r_{1b}}^2} = \frac{K_T}{{r_{1b}}^2} \tag{3.7}$$

Linear tooth mesh stiffness is given by the ratio of torsional tooth mesh stiffness and square of base circle radius of the gear 1.

$$K_m = \frac{K_T}{{r_{1b}}^2} \tag{3.8}$$

3.1.2 Modeling of Spur Gear Using Inventor Professional 2016

Model must be created by using appropriate dimensions, boundary conditions (constraints), forces, selection of appropriate mesh, element choice, etc. There two methods to construct finite element model. One of that method includes the creation of Computer Aided Design model using modeling softwares such as Solidworks, or CATIA and export a model to ANSYS Workbench with appropriate file formats such as IGES or Parasolid for analysis. The another method includes modeling using any analysis software to build that particular model. The basic disadvantage of this method is that user can not generate a complex model easily.

In this work, Inventor professional 2016 used to create a model of the spur gear pair and ANSYS Workbench 15.0 is used for the Finite Element Analysis of this gear system. Basically, this analysis has been done to calculate the meshing stiffness between meshing gear pairs like sun gear and planet as well as planet and ring gear. They are afterwards compared with the analytical methods (spott's equation).

Model is constructed using the dimensions shown in Table 3.1

All dimensions are in mm

Pressure angle = 20°

Table 3.1: Parameters used to create epicyclic gear in Inventor professional 2016

Parameters	Sun Gear	Planet	Ring Gear
Pitch Circle Diameter (d)	160	220	600
Base Circle Diameter(d_b = d X cos(PA))	150.351	206.732	563.816
Number of teeth,(N)	16	22	60
Diametral Pitch ,(P)	0.1	0.1	0.1
Addendum , (a =1/P)	10	10	10
Outside Diameter , (d_o = d +2a)	180	240	620
Circular Pitch , (p = 3.1416/P)	31.416	31.416	31.416
Whole Depth, (ht = 2.157/P)	21.57	21.57	21.57
Deddendum ,(ded = ht –a)	11.57	11.57	11.57
Root Diameter ,(d_r = d -2b)	136.86	196.86	576.86
Tooth width,(b)	10	10	10

CAD model for the epicyclic gear was constructed. It includes one spur gear, one planet gear, one ring gear and the carrier. This model was created using the 'Inventor Professional 2016'.

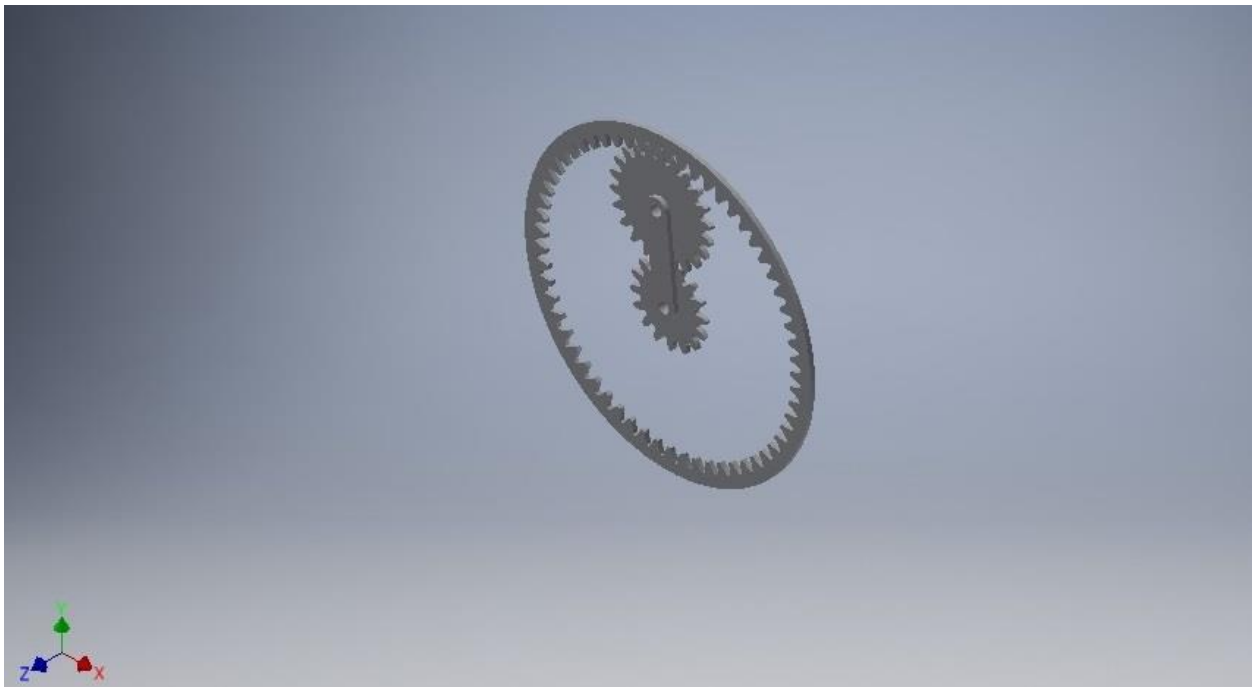

Figure 3.3: CAD model: Epicyclic Gear Set

3.1.3 Various Boundary Conditions, Applied Loads and Displacements

Boundary conditions are applied to the various components like rotational degree of freedom is given to the one whose displacement we have to calculate. While the other meshing component is fixed so that it creates the stress and the strain fields. Fig. 3.4 gives the general idea about the meshing gears and applied boundary conditions.

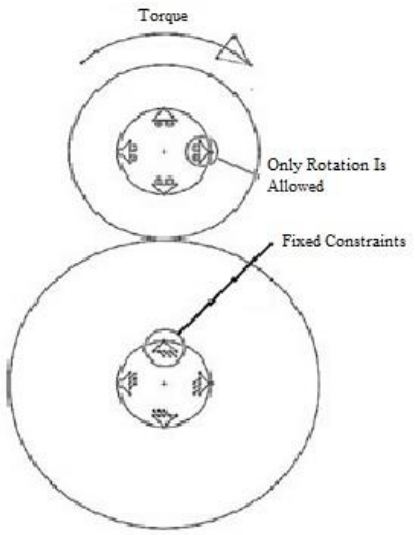

Figure 3.4: Boundary conditions and applied load (input torque) for the analysis

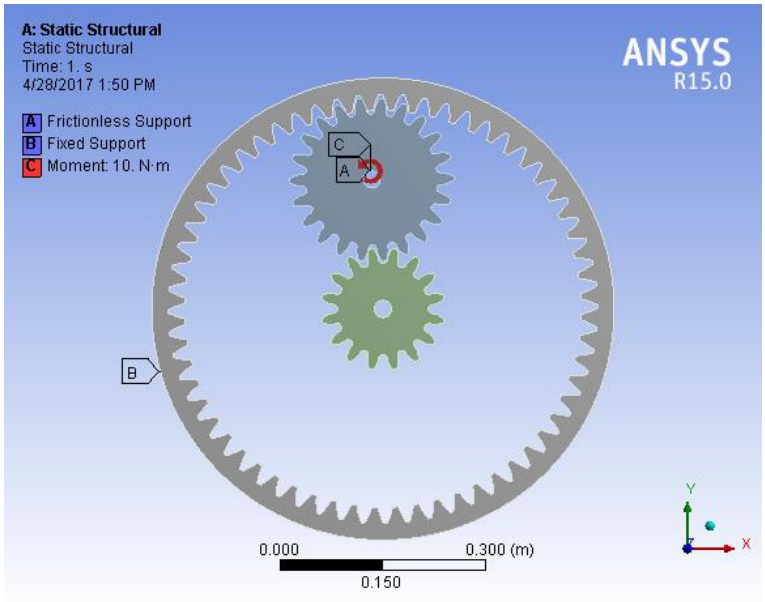

Figure 3.5: Boundary conditions in ANSYS Workbench 15.0 for ring-planet mesh

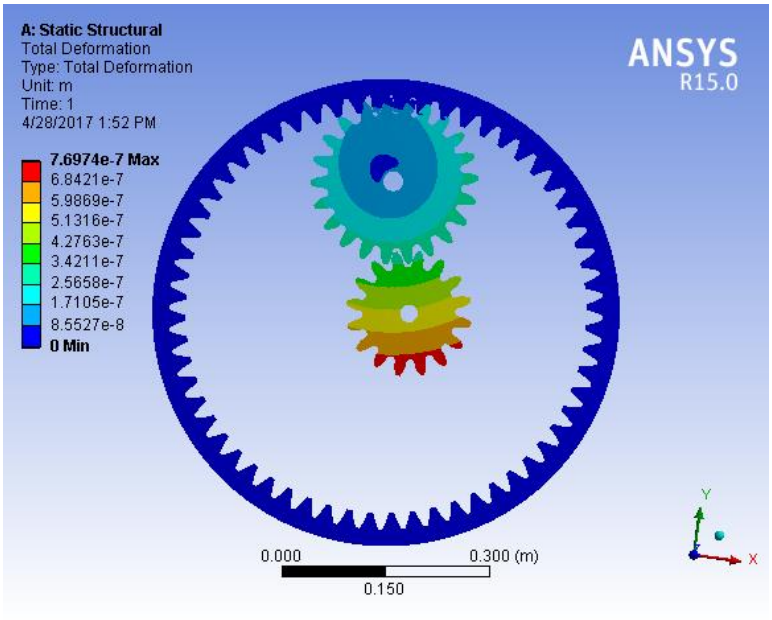

Figure 3.6: Displacement field in ANSYS Workbench 15.0 for ring-planet mesh

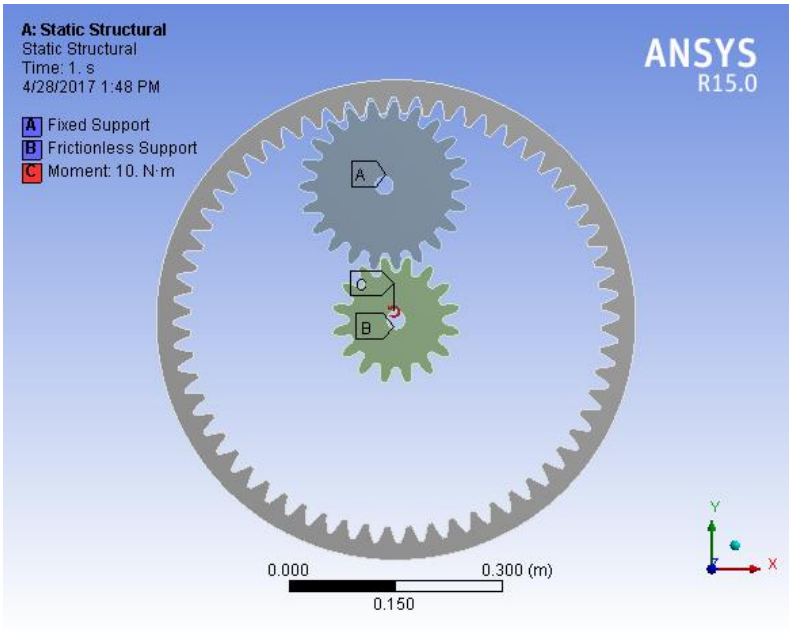

Figure 3.7: Boundary conditions in ANSYS Workbench 15.0 for sun-planet mesh

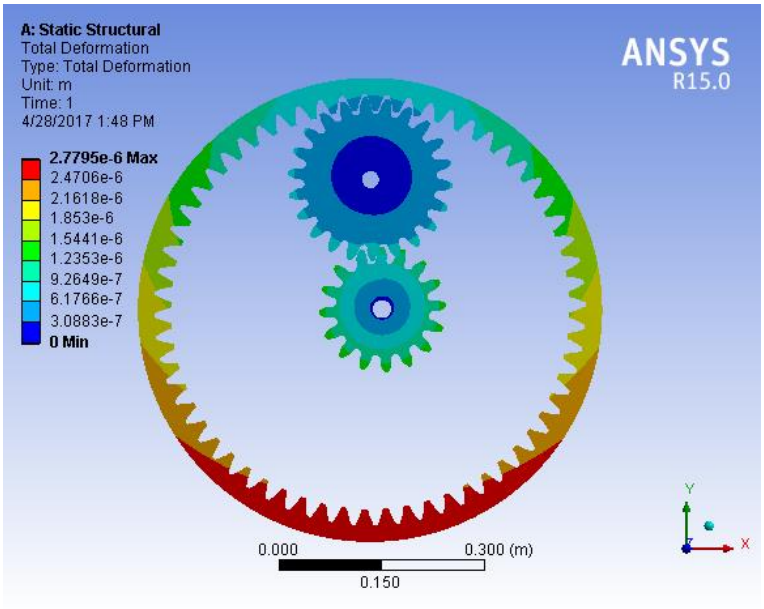

Figure 3.8: Displacement field in ANSYS Workbench 15.0 for sun-planet mesh

Above boundary conditions have been applied to obtain a result in Ansys workbench 15.0. Displacement field in the Ansys is used to calculate the mesh stiffness for the given ring-planet pair as well as sun-planet pair in the epicyclic gear.
Displacement field is calculated:
Applied moment= 10Nm

3.1.4 Results and Comparison

3.1.4.1 Ring-planet mesh

Planet Gear Dimensions (For calculations)
Addendum radius, r_a = 240 mm
Base circle radius, r_b = 206.732 mm
Torque applied T = 10 Nm

Calculations:

Displacement of the planet gear (s): 0.516 X 10^{-6} m

Angular displacement ($\theta = \frac{S}{r_a}$): $\frac{0.516\ X\ 10-6}{0.240}$ = 2.15 X 10^{-6} rad

Torsional Stiffness ($K_t = \frac{T}{\theta}$): $\frac{10}{2.15\ X\ 10-6}$ = 4.651163 X 10^{6} Nm/rad

Mesh stiffness ($K_m = \frac{K_t}{{r_b}^2}$): $\frac{4.651163\ X\ 106}{0.206732^2}$ = 108.83 X 10^{6} N/m

3.1.4.2 Sun-planet mesh

Sun Gear Dimensions (For calculations)
Addendum radius, r_a = 180 mm
Base circle radius, r_b = 150.351 mm
Torque applied T = 10 Nm

Calculations:

Displacement of the planet gear (s): 0.75 X 10^{-6} m

Angular displacement ($\theta = \frac{S}{r_a}$): $\frac{0.75\ X\ 10-6}{0.180}$ = 4.16667 X 10^{-6} rad

Torsional Stiffness ($K_t = \frac{T}{\theta}$): $\frac{10}{4.16667\ X\ 10-6}$ = 2.4 X 10^6 Nm/rad

Mesh stiffness ($K_m = \frac{K_t}{{r_b}^2}$): $\frac{2.4\ X\ 106}{0.150351^2}$ = 106.17 X 10^6 N/m

3.1.4.3 Comparison

Calculated results are compared with the Spotts (1985) equation, which states average the mesh stiffness of the gear pair.

Average gear mesh stiffness obtained:

1. Ring-planet mesh:

$$K_m = 108.83 \text{ MN/m}$$

2. Sun-planet mesh:

$$K_m = 106.17 \text{ MN/m}$$

3. By using Spott's equation of average mesh stiffness:

$$K_m = \frac{b}{9} * \frac{E_1 * E_2}{E_1 + E_2} \quad (3.9)$$
$$= 111.11 \text{ MN/m}$$

Where,

E_1 = Elastic modulus of 1st gear = 200 GPa

E_2 = Elastic modulus of 2nd gear = 200 GPa

4. By using modified Spotts equation of average mesh stiffness:

$$K_m = C.R. * \frac{b}{9} * \frac{E_1 * E_2}{E_1 + E_2} \quad (3.10)$$

I. Ring-planet mesh:

$$K_m = 1.55 \text{ X } 111.111$$
$$= 172.22 \text{ MN/m}$$

Where,

C.R. = Contact ratio = 1.55

II. Sun-planet mesh:

$$K_m = 1.40 \text{ X } 111.111$$
$$= 155.55 \text{ MN/m}$$

Where,

C.R. = Contact ratio = 1.40

From the above calculations, it is concluded that Spotts equation for mesh stiffness can be used to calculate the mesh stiffness of the given gear pair and it gives an approximate value of the mesh stiffness.

4 Gear-Mesh Model Methodology with Application

This chapter has the methodology for deriving 6 order mesh stiffness matrices for each meshing pair like sun-planet, ring-planet as well as carrier-planet. This approach used technique proposed by Lao (1996) and it also includes some aspects presented by Choi (1993) and Blankenship (1995). Mesh stiffness matrices for each pair are derived by resolving forces and displacement of a pitch point.

4.1 Gear Mesh Model Methodology

4.1.1 Development of Gear Mesh Forcing Function

Figure 4.1 represents the finite element system of the meshing gear with shafts.

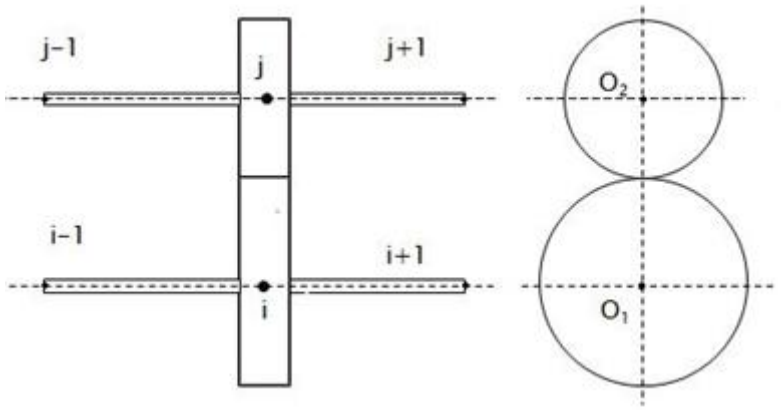

Figure 4.1: Finite element representation of a Gear Pair

Both the gears act as rigid disks on shafts. Two centers of the respective gears act as separate nodes for the finite element analysis. A force vector {F} can be modeled as function of a gear mesh stiffness matrix $[K]_{mesh}$ and displacement vector {q} acts on a node i and j.

$$\begin{Bmatrix} F_i \\ F_j \end{Bmatrix} = [K]_{mesh} \begin{Bmatrix} q_i \\ q_j \end{Bmatrix} = K_m \begin{bmatrix} [K_{ii}] & [K_{ij}] \\ [K_{ji}] & [K_{jj}] \end{bmatrix} \begin{Bmatrix} q_i \\ q_j \end{Bmatrix} \quad (4.1)$$

4.1.2 Geometry and Loading Conditions

The mesh between two gears is represented by a spring mass system. Line of action is the path along which the force between these two gears is transmitted and it is given by the tangent joining the base circles of the two meshing gears.

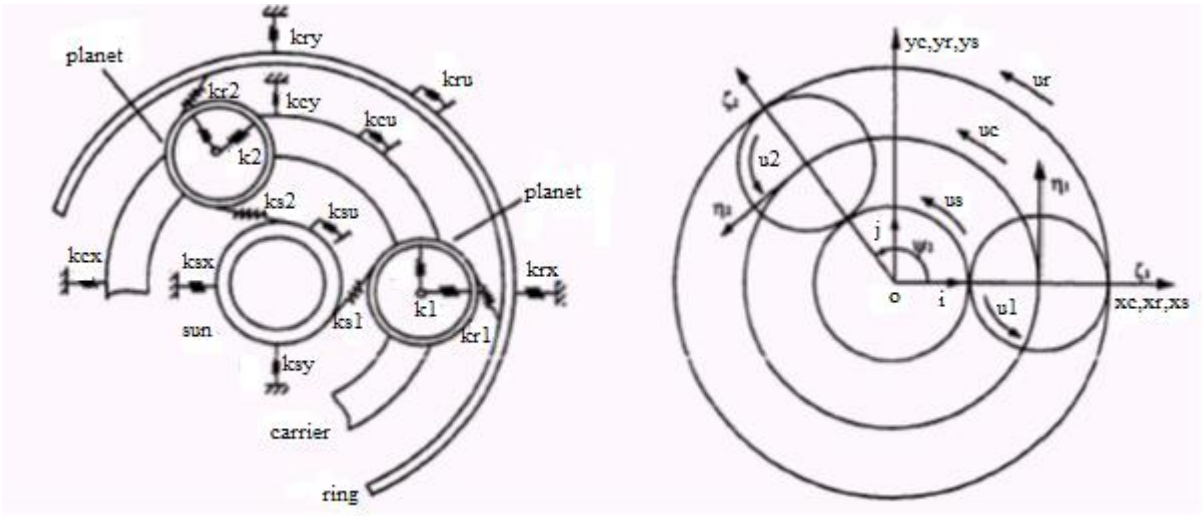

Figure 4.2: Epicyclic Gear Model

The intersection of two lines, lines connecting two centers of the given gear pair and the tangents connecting two base circles (Line of Action) gives the pitch point. In spur gears, contact load is distributed evenly, not like helical gears in which the contact area varies accordingly and hence the transmitted load. The force transmission is assumed to be taking place at the pitch point p.

Location of the given gear pair is taken into account using the variable. If the given gear pair is horizontal, it is given as, ht= 0 and if the given gear pair is arranged vertically, ht= r_i+r_j or at any given orientation φ.

In this method, the mesh stiffness value for the given meshing gear pair is assumed to be derived from the experimental results or can be calculated from the documented data of the given system. It basicaaly depends on the materials of two meshing gears. The whole geometry of each meshing gear pair can be explained and related using the given variables: Orientation angle (φ) and the pressure angle (α).

In the case of the spur gear, problem can be solved in two dimensions or x-y plane by ressolving the forces. Force components are basically the functions of the pressure angle (α) and these local force components are related with the global components using the orientation angle (φ).

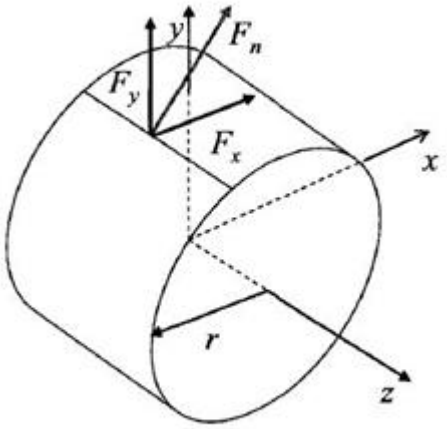

Figure 4.3: Forces acting on the spur gear

The local forces are the function of the direction cosines. Direction cosine angles can be written in the form the pressure angle (α). The force components along x' and y' and axes are determined by equations 5.2. The role of prime coordinates (x' and y') is very vital.

$$F_{x'} = F_n \cos\phi_x$$

$$F_{y'} = F_n \cos\cos\phi_y \qquad (4.2)$$

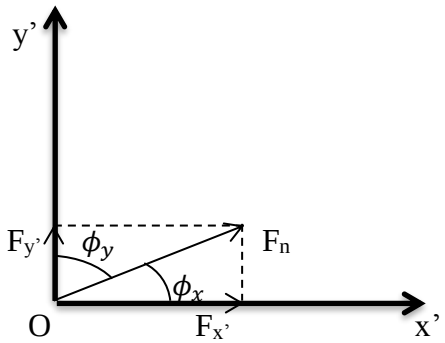

Figure 4.4 Force Components

Where,

$$\cos\phi_x = \cos\beta \cos\alpha$$
$$\cos\phi_y = \sin\alpha \qquad (4.3)$$
$$\cos\phi_z = 0$$

The equation relating the force vector to displacement vector is

$$\{F\}_{mesh} = -[K]_{mesh}\{u\}_{LOA} \tag{4.4}$$

Forces in the global coordinate system is brought to the left hand, so the negative sign is present.

4.1.3 Gear-Mesh Coordinates System

The coordinate axes (x' as well as y') are local to the pitch point. It is shown in the figure. The orientation angle (φ) decides the direction of these prime coordinates. While, the pressure angle decides the force components. In the case of epicyclic gear, the orientation angle keeps changing for each sun-planet gear. It keeps rotating about the gear center i.

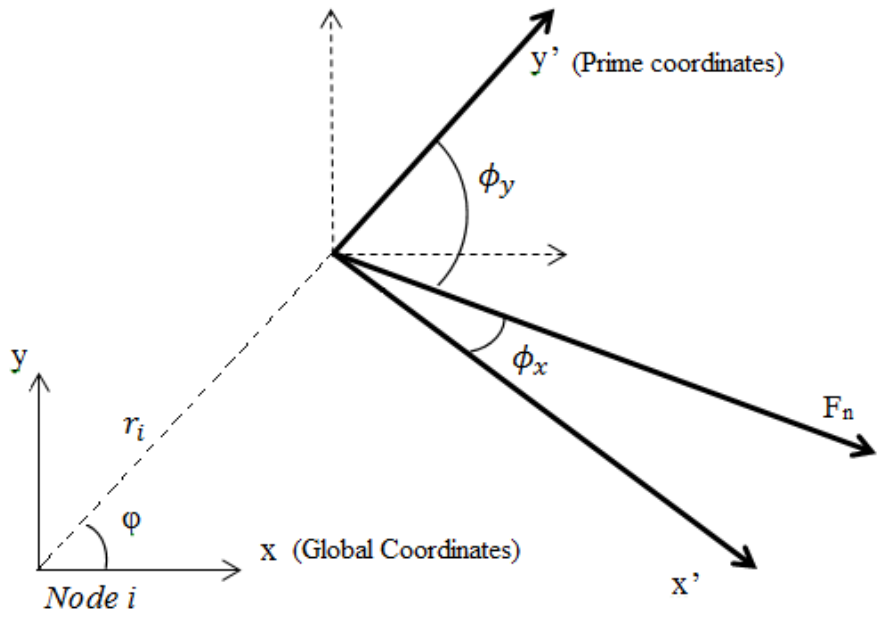

Figure 4.5: Relation between Local and Global Axes

As shown above, prime coordinates can be resolved in both the global x as well as y axes. Similarly, forces have the components in the global axes accordingly. Afterwards, these can be related accordingly to find out the stifness matrices for each meshing pair.

4.1.4 Force and Moment Equations

The foces acting on the node i, can be resolved in the x and y (global axes) direction. While, the moment can be found out by multiplying the respective forces with their moment arm around the given node. As in the spur gear, there is no force acting in the axial direction, F_z in not present. The moments about the global x and y axes contain the force term F_z, so they are absent as well.

$$\begin{aligned} F_{xi} &= F_x, \sin\varphi + F_y, \cos\varphi \\ F_{yi} &= -F_x, \cos\varphi + F_y, \sin\varphi \\ F_{zi} &= 0 \end{aligned} \tag{4.5}$$

Moments,

$$\begin{aligned} M_{xi} &= 0 \\ M_{yi} &= 0 \\ M_{zi} &= F_{yi}\, r_i \cos\varphi - F_{xi}\, r_i \sin\varphi \end{aligned} \tag{4.6}$$

The forces acting on the j node are equal in the magnitude and opposite to those acting on the i node. While the moments are equal and opposite only if the gear ratio is unity. So, the forces and moments acting on the meshing j node of the gear pair are given as:

$$\begin{aligned} F_{xj} &= -(F_x, \sin\varphi + F_y, \cos\varphi) \\ F_{yj} &= -(-F_x, \cos\varphi + F_y, \sin\varphi) \\ F_{zj} &= 0 \end{aligned} \tag{4.7}$$

$$\begin{aligned} M_{xj} &= 0 \\ M_{yj} &= 0 \\ M_{zj} &= F_{yj}\, r_j \cos\varphi - F_{xj}\, r_j \sin\varphi \end{aligned} \tag{4.8}$$

4.1.5 Displacement Method

4.1.5.1 Sun-Planet Mesh (Forces on the sun gear)

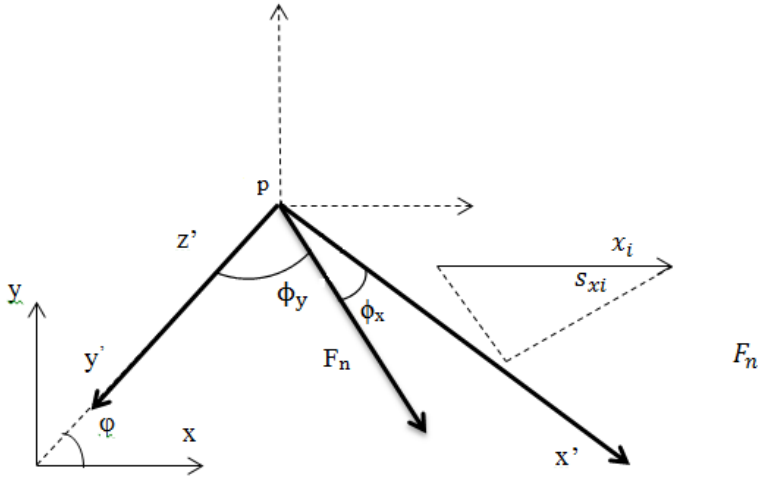

Figure 4.6: Contribution of displacements to the Line-of-Action (sun-planet mesh)

There are total 6 DOF per gear pair mesh. They all contribute to the movement of the pitch point along the 'Line of Action'. Positive displacements of the nodes i and j of the respective gears along the x-direction result in the components along the line of action.

The pitch point gets shifted due to these translational moctions along the given axes. Rotational motion about an axis rotates pitch point about the respective axes.

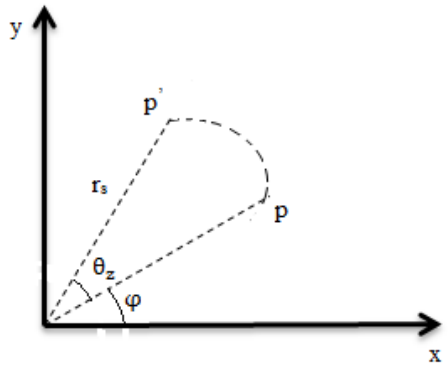

Figure 4.7: Contribution of the rotational motion about z_i in the movment of the pitch point

The displacement method is applied to the each meshing gear pair in the epicyclic gear train which yields the 6 X 6 mesh stiffness matrix for each meshing pair. The pitch point

displacement can be resolved into the global coordinate system using the appropriate transformations. The pressure angle (α) helps to resolve the components along the prime (local) coordinate system while the orientation angle (φ) gives the relationship between the prime and global coordiante system. The applied displacement method gives the following equations:

$$\begin{aligned} s_{xs} &= x_s\left(\sin\varphi\cos\phi_x - \cos\varphi\cos\phi_y\right) \\ &= x_s \sin\varphi_s \qquad \ldots\ldots \quad (\varphi_s = \varphi - \alpha_s) \end{aligned} \tag{4.9}$$

$$\begin{aligned} s_{ys} &= y_s\left(-\sin\varphi\cos\phi_y - \cos\varphi\cos\phi_x\right) \\ &= -y_s \cos\varphi_s \end{aligned} \tag{4.10}$$

The rotational displacement:

For rotation about z axis:

$$x_s = -r_s\cos\varphi + r_s\cos(\varphi + \theta_{zs}) \tag{4.11}$$

$$y_s = -r_s\sin\varphi + r_s\sin(\varphi + \theta_{zs}) \tag{4.12}$$

Due to the small rotating angle assumption,

For rotation about (z):

$$x_s = -r_s\theta_{zs}\sin(\varphi) \tag{4.13}$$

$$y_s = +r_s\theta_{zs}\cos(\varphi) \tag{4.14}$$

By substituting these equations into the translational displacement equation we get,

$$s_{\theta zs} = -r_s\theta_{zs}\cos\alpha_s \tag{4.15}$$

Forces acting on the sun gear are:

$$\begin{aligned} F_x &= F_n \sin\varphi_s \\ F_y &= F_n \cos\varphi_s \\ M_z &= -F_n r_s \cos\alpha_s \end{aligned} \tag{4.16}$$

4.1.5.2 Ring-Planet Mesh (Forces on the ring gear)

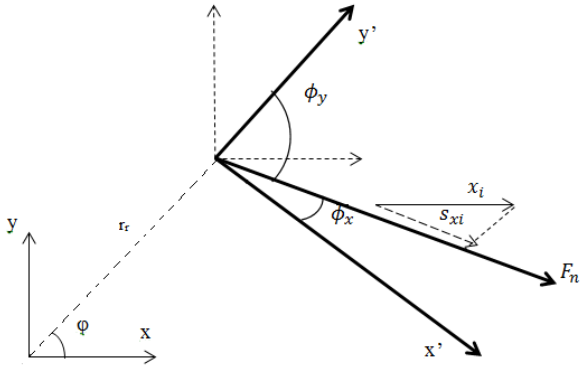

Figure 4.8: Contribution of displacements to the Line-of-Action (ring-planet mesh)

Similar procedure is applied for the ring-planet mesh,

The applied displacement method gives the following equations:

$$s_{xr} = x_r(\sin\varphi\cos\phi_x + \cos\varphi\cos\phi_y)$$
$$= -x_r \sin\varphi_r \quad \ldots\ldots \quad (\varphi_r = \varphi + \alpha_r) \tag{4.17}$$

$$s_{yr} = y_r(-\sin\varphi\cos\phi_y + \cos\varphi\cos\phi_x)$$
$$= -y_r \cos\varphi_r \tag{4.18}$$

The rotational displacement:

For rotation about z axis:

$$x_r = -r_r\cos\varphi + r_r\cos(\varphi + \theta_{zr}) \tag{4.19}$$

$$y_r = -r_r\sin\varphi + r_r\sin(\varphi + \theta_{zr}) \tag{4.20}$$

Due to the small rotating angle assumption,

For rotation about (z):

$$x_r = -r_r\theta_{zr}\sin(\varphi) \tag{4.21}$$

$$y_r = +r_r\theta_{zr}\cos(\varphi) \tag{4.22}$$

By substituting these equations into the translational displacement equation we get,

$$s_{\theta zr} = -r_r \theta_{zr} \cos\alpha_r \tag{4.23}$$

Forces acting on the ring gear are:

$$F_x = F_n \sin \varphi_r$$

$$F_y = F_n \cos \varphi_r$$

$$M_z = - F_n r_r \cos \alpha_r \tag{4.24}$$

4.1.5.3 Carrier-Planet Mesh (Forces on the carrier)

4.1.5.3.1 Vertical Force Acting on the Carrier

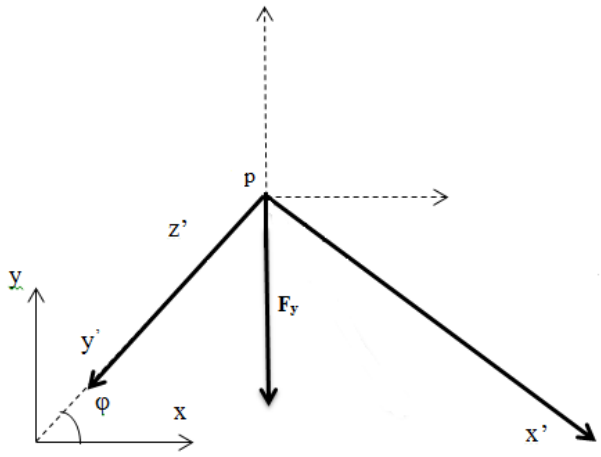

Figure 4.9: Contribution of vertical force to pitch point movement (carrier-planet mesh)

Similar procedure is applied for the carrier-planet mesh,

The applied displacement method gives the following equations:

$$s_{xcy} = x_{cy}(\sin\varphi\cos\varphi - \cos\varphi\sin\varphi) = 0 \tag{4.25}$$

$$s_{ycy} = y_{cy}(-\sin\varphi\sin\varphi - \cos\varphi\cos\varphi) = -y_{cy} \tag{4.26}$$

The rotational displacement:

For rotation about z axis:

$$x_{cy} = -r_c\cos\varphi + r_c\cos(\varphi + \theta_{zcy}) \tag{4.27}$$

$$y_{cy} = -r_c\sin\varphi + r_c\sin(\varphi + \theta_{zcy}) \tag{4.28}$$

Due to the small rotating angle assumption,

For rotation about (z):

$$x_{cy} = -r_c\theta_{zcy}\sin(\varphi) \tag{4.29}$$

$$y_{cy} = +r_c\theta_{zcy}\cos(\varphi) \tag{4.30}$$

By substituting these equations into the translational displacement equation we get,

$$s_{\theta zc} = -r_c\theta_{zcy}\cos(\varphi) \tag{4.31}$$

Forces acting on the carrier are:

$$F_x = 0$$

$$F_y = -F_y$$

$$M_z = 0$$

(As carrier rotation has no rotational effect on the pitch point movement) (4.32)

4.1.5.3.2 Horizontal Force Acting on the Carrier

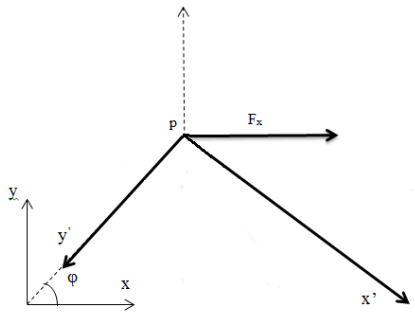

Figure 4.10: Contribution of horizontal force to pitch pt movement (carrier-planet mesh)

The applied displacement method gives the following equations:

$$\begin{aligned} s_{xcx} &= x_{cx}(\sin\varphi\sin\varphi + \cos\varphi\cos\varphi) \\ &= x_{cx} \\ s_{xp} &= -x_{px} \end{aligned} \tag{4.33}$$

$$\begin{aligned} s_{ycx} &= y_{cx}(-\sin\varphi\cos\varphi + \cos\varphi\sin\varphi) \\ &= 0 \end{aligned} \tag{4.34}$$

The rotational displacement:

For rotation about z axis:

$$x_{cx} = -r_c\cos\varphi + r_c\cos(\varphi + \theta_{zcx}) \tag{4.35}$$

$$y_{cx} = -r_c\sin\varphi + r_c\sin(\varphi + \theta_{zcx}) \tag{4.36}$$

Due to the small rotating angle assumption,

For rotation about (z):

$$x_{cx} = -r_c\theta_{zcx}\sin(\varphi) \tag{4.37}$$

$$y_{cx} = +r_c\theta_{zcx}\cos(\varphi) \tag{4.38}$$

By substituting these equations into the translational displacement equation we get,

$$s_{\theta zc} = -r_c\theta_{zcx}\sin(\varphi) \tag{4.39}$$

Forces acting on the carrier are:

$$F_x = F_x$$

$$F_y = 0$$

$$M_z = 0$$

(As carrier rotation has no rotational effect on the pitch point movement) (4.40)

4.1.5.4 Sun-Planet Mesh (Forces on the planet gear)

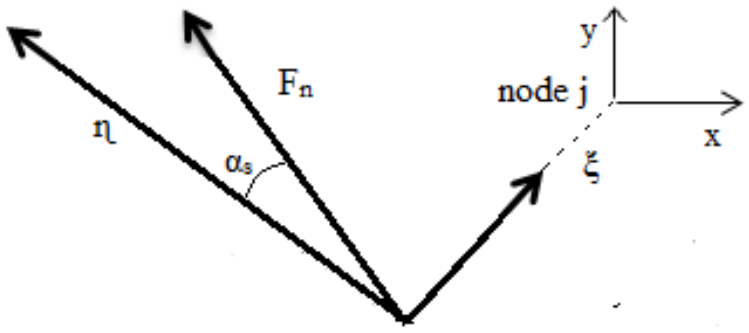

Figure 4.11: Force on the planet gear due to sun-planet mesh

The applied displacement method gives the following equations:

(As, linear displacements due to node i and j are the same)

$$s_\xi = -\xi(\sin\alpha_s) \tag{4.41}$$

$$s_\eta = -\eta(\cos\alpha_s) \tag{4.42}$$

For rotation about (z):

$$s_{\theta zp} = -r_p\theta_{zp}\cos\alpha_s \tag{4.43}$$

Forces acting on the sun gear are:

$$F_\xi = F_n \sin\alpha_s$$

$$F_\eta = F_n \cos\alpha_s$$

$$M_z = -F_n\, r_p \cos\alpha_s \tag{4.44}$$

4.1.5.5 Ring-Planet Mesh (Forces on the planet gear)

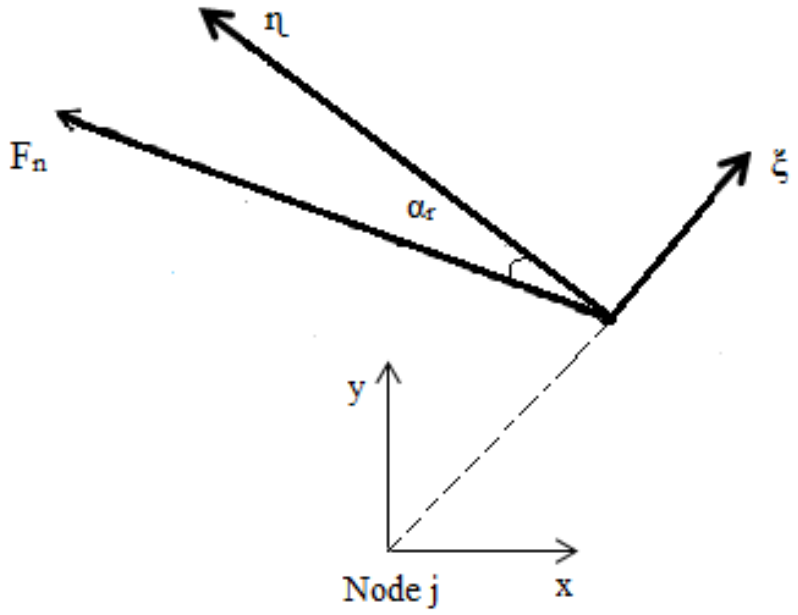

Figure 4.12: Force on the planet gear due to ring-planet mesh

The applied displacement method gives the following equations:

(As, linear displacements due to node i and j are the same)

$$s_\xi = \xi(\sin\alpha_r) \tag{4.45}$$

$$s_\eta = -\eta(\cos\alpha_r) \tag{4.46}$$

For rotation about (z):

$$s_{\theta zp} = r_p\theta_{zp}\cos\alpha_r \tag{4.47}$$

Forces acting on the sun gear are:

$$F_\xi = -F_n \sin\alpha_r$$

$$F_\eta = F_n \cos\alpha_r$$

$$M_z = F_n\, r_p \cos\alpha_r \tag{4.48}$$

4.1.5.6 Carrier-Planet Mesh (Forces on the planet gear)

4.1.5.6.1 Vertical Force Acting on the Planet

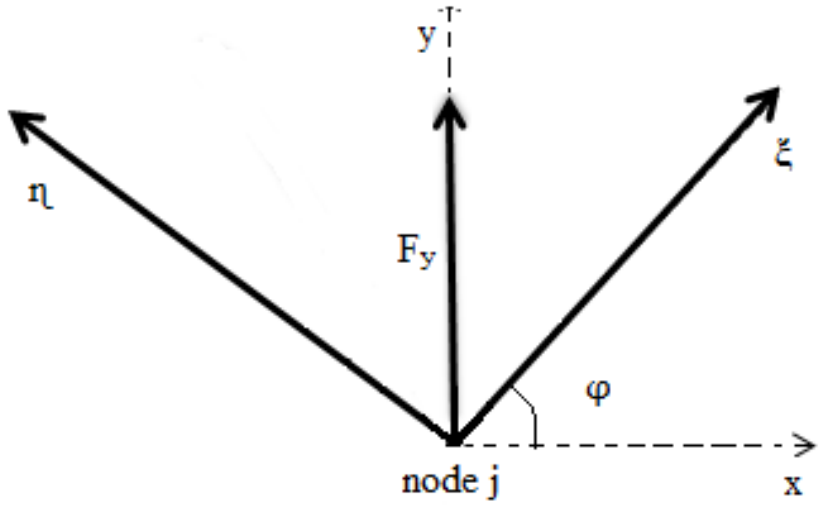

Figure 4.13: Vertical force on the planet gear due to carrier

The applied displacement method gives the following equations:

(As, linear displacements due to node i and j are the same)

$$s_\xi = -\xi(\sin\varphi) \tag{4.49}$$

$$s_\eta = -\eta(\cos\varphi) \tag{4.50}$$

For rotation about (z):

$$s_{\theta zp} = 0 \tag{4.51}$$

Forces acting on the sun gear are:

$$F_\xi = F_y \sin\varphi$$

$$F_\eta = F_y \cos\varphi$$

$$M_z = 0 \tag{4.52}$$

4.1.5.6.2 **Horizontal Force Acting on the Planet**

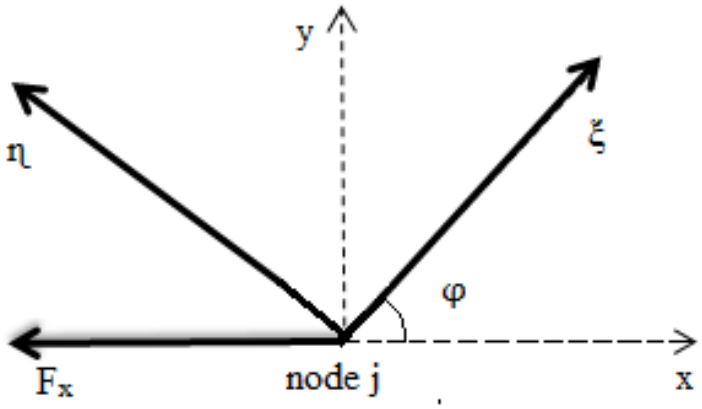

Figure 4.14: Horizontal force on the planet gear due to carrier

The applied displacement method gives the following equations:

(As, linear displacements due to node i and j are the same)

$$s_\xi = \xi(\cos\varphi) \tag{4.53}$$

$$s_\eta = -\eta(\sin\varphi) \tag{4.54}$$

For rotation about (z):

$$s_{\theta zp} = 0 \tag{4.55}$$

Forces acting on the sun gear are:

$$F_\xi = -F_x \cos\varphi$$

$$F_\eta = F_x \sin\varphi$$

$$M_z = 0 \tag{4.56}$$

This procedure can be repeated for n number of the meshing planet gears. Applying the same formulation method, suitable stiffness matrices can be found out. The only varying element present is the orientation angle and the realted terms.

4.1.6 Influence Coeffiecient Method

Each element of the mesh stiffness matrix for each meshing pair can be calculated by assuming only one component of displacement vector {q} has a unit displacement, and all the other remaining components of the displacement vector $\{q_i\}$ and $\{q_j\}$ are zero. Then we put the values of F_n in term of force vector components. Negative value of force vector component represents the particulat element stiffness value. By applying each of three different unit displacements in $\{q_i\}$ will yield a 3×6 matrix. Similarly, using the same method to each of the variables in $\{q_j\}$ yields another 3×6 matrix. Combining all these matrices, we can get a matrix of 6x6.
It can be written as,

$$[K]_{mesh} = K_m \begin{bmatrix} [K_{ii}] & [K_{ij}] \\ [K_{ji}] & [K_{jj}] \end{bmatrix} \tag{4.57}$$

The element of the four submatrices in Equation 4.57 for each meshing pair are presented in Appendix B

4.1.7 Finding out the meshing frequency

The meshing frequency for the given system can be found out in such a way that the whole system (carrier, ring, sungear, planet 1, planet 2, ……, planet n)displacement parameters are arranged and matched up with the meshing matrix.

$$K_m = \begin{bmatrix} \sum_{i=1}^{n} [Kc_1]^i & 0 & 0 & [Kc_2]^1 & [Kc_2]^2 & [Kc_2]^3 & [Kc_2]^4 \\ 0 & \sum_{i=1}^{n} [Kr_1]^i & 0 & [Kr_2]^1 & [Kr_2]^2 & [Kr_2]^3 & [Kr_2]^4 \\ 0 & 0 & \sum_{i=1}^{n} [Ks_1]^i & [Ks_2]^1 & [Ks_2]^2 & [Ks_2]^3 & [Ks_2]^4 \\ [Kc_3]^1 & [Kr_3]^1 & [Ks_3]^1 & [Kpp]^1 & 0 & 0 & 0 \\ [Kc_3]^2 & [Kr_3]^2 & [Ks_3]^2 & 0 & [Kpp]^2 & 0 & 0 \\ [Kc_3]^3 & [Kr_3]^3 & [Ks_3]^3 & 0 & 0 & [Kpp]^3 & 0 \\ [Kc_3]^4 & [Kr_3]^4 & [Ks_3]^4 & 0 & 0 & 0 & [Kpp]^4 \end{bmatrix} \tag{4.58}$$

The above sub-matrices are given in the Appendix A.

4.2 Application

4.2.1 System and System Parameter

The formulated meshing stiffness matrices for the given epicyclic system can be incorporated in the finding out the natural frequency of the system. The formulation in this paper is used to verify the meshing frequencies of the system used in the U.S. Army's helicopter OH-58.

Table 4.1: System Parameters

Parameters	Sun	Ring	Carrier	Planet
Mass (kg)	0.4	2.35	5.43	0.66
$\mathbf{I}/\mathbf{r^2}$ (kg)	0.39	3.00	6.29	0.61
Base Diameter (mm)	77.42	275.03	177.8	100.35
Teeth Number	27	99		35
Mesh Stiffness ($\mathbf{N}/\mathbf{m}$)	$k_{sp} = k_{rp} = k_m = 5 \times \mathbf{10^8}$			
Beating Stiffness ($\mathbf{N}/\mathbf{m}$)	$k_p = k_s = k_r = k_c = \mathbf{10^8}$			
Torsion Stiffness ($\mathbf{N}/\mathbf{m}$)	$k_{ru} = \mathbf{10^9}$, $k_{su} = k_{cu} = \mathbf{10^9}$			
Pressure Angle (º)	$\alpha_s = \alpha_r = 24.6$			

4.2.2 Results of Meshing Epicyclic Gears

Natural Frequency results obtained using the MATLAB software are:

Table 4.2: Natural Frequencies (Hz) of Meshing Epicyclic Gears

Multiplicity	Mode	Natural Frequency (Hz)	Frequency Number
m=1	Pure Rotation of Carrier, Ring and Sun	0	1
		1536.5	6
		1970.6	10
		2625.7	13
		7773.6	18
		13071	21
m=2	Pure Translation of Carrier, Ring and Sun	727.27	2,3
		1091.2	4,5
		1892.8	8,9
		2342.5	11,12
		7189.9	16,17

		10458	19,20
m=1	Planet Modes	1808.28	7
		5963.8	14
		6981.7	15

4.2.3 Validation

These obtained natural frequencies are compared and validated with th previous study by J. Lin and R. G. Parker. Comparison of these natural frequencies is given in the following table. From the comparison, it is given that the method developed for the formulation of the meshing stiffness matrices and hence the meshing frequencies gives the exact same results.

Table 4.3: Comparison of Natural Frequencies

Natural Frequecy Number	Frequecy by J. Lin and R. G. Parker (Hz)	Calculated Natural Frequency (Hz)	Difference (%)
1	0	0	0.00
2,3	727.0	727.27	0.037
4,5	1091.0	1091.2	0.018
6	1536.6	1536.5	0.007
7	1808.2	1808.28	0.004
8,9	1892.8	1892.8	0.00
10	1970.6	1970.6	0.00
11,12	2342.5	2342.5	0.00
13	2625.7	2625.7	0.00
14	5963.8	5963.8	0.00
15	6981.7	6981.7	0.00

16,17	7189.9	7189.9	0.00
18	7773.6	7773.6	00.00
19,20	10437.6	10438	0.004
21	13071.1	13071	0.001

5 Results

Natural frequencies help us to understand the system behavior in details.

5.1 Mode Shapes

The obtained natural frequencies can be divided in the following categories:

i. Rotational Modes: These modes have multiplicity m=1 for the given system. That implies that these modes don't repeat themselves. The related vibration modes have pure rotation of carrier, ring and sun. While planets have the same motion.

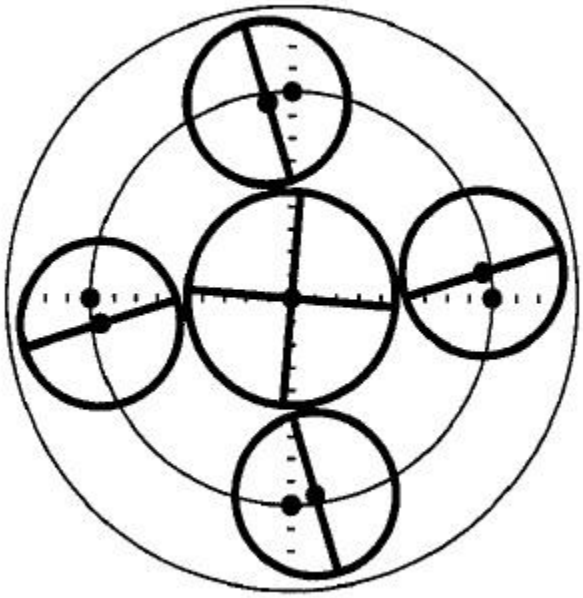

Figure 5.1: Rotational Mode (R. G. Parker and J. Lin)

Table 5.1: Rotational Mode Natural Frequencies

Multiplicity	1					
Frequency No.	1	6	10	13	18	21
Frequency (Hz)	0	1536.5	1970.6	2625.7	7773.6	13071

Table 5.2: Rotational Mode Shapes (Matlab)

Frequency No.	1	6	10	13	18	21
Mode Shapes						
Carrier						
X Disp	-0.0000	-0.0000	0.0000	-0.0000	-0.0000	0.0000
Y Disp	0.0000	0.0000	-0.0000	-0.0000	0.0000	0.0000
Rotational Disp	-0.5499	-0.5752	0.2419	-0.2220	-0.0274	0.0012
Ring						
X Disp	-0.0000	-0.0000	-0.0000	-0.0000	-0.0000	-0.0000
Y Disp	-0.0000	0.0000	0.0000	0.0000	0.0000	0.0000
Rotational Disp	0.0000	-0.3637	0.1074	1.0000	-0.9863	-0.0096
Sun						
X Disp	0.0000	0.0000	0.0000	0.0000	-0.0000	0.0000
Y Disp	0.0000	-0.0000	0.0000	0.0000	0.0000	-0.0000
Rotational Disp	-1.0000	1.0000	-0.7802	0.2456	-0.4326	1.0000
Planet 1						
Radial Disp	0.0000	-0.6103	-1.0000	-0.2739	-0.4002	-0.0673
Tangential Disp	-0.5499	0.2678	-0.3412	0.7283	1.0000	-0.1278
Rotational Disp	0.5000	-0.9924	0.0303	0.3156	0.9740	0.1711
Planet 2						
Radial Disp	0.0000	-0.6103	-1.0000	-0.2739	-0.4002	-0.0673
Tangential Disp	-0.5499	0.2678	-0.3412	0.7283	1.0000	-0.1278
Rotational Disp	0.5000	-0.9924	0.0303	0.3156	0.9740	0.1711
Planet 3						
Radial Disp	0.0000	-0.6103	-1.0000	-0.2739	-0.4002	-0.0673
Tangential Disp	-0.5499	0.2678	-0.3412	0.7283	1.0000	-0.1278
Rotational Disp	0.5000	-0.9924	0.0303	0.3156	0.9740	0.1711
Planet 4						
Radial Disp	0.0000	-0.6103	-1.0000	-0.2739	-0.4002	-0.0673
Tangential Disp	-0.5499	0.2678	-0.3412	0.7283	1.0000	-0.1278
Rotational Disp	0.5000	-0.9924	0.0303	0.3156	0.9740	0.1711

ii. Translational Modes: These modes have multiplicity m=2 for the given system. The related vibration modes have pure translational displacement of carrier, ring and sun. While all the planets have radial, tangential as well as the rotational displacement.

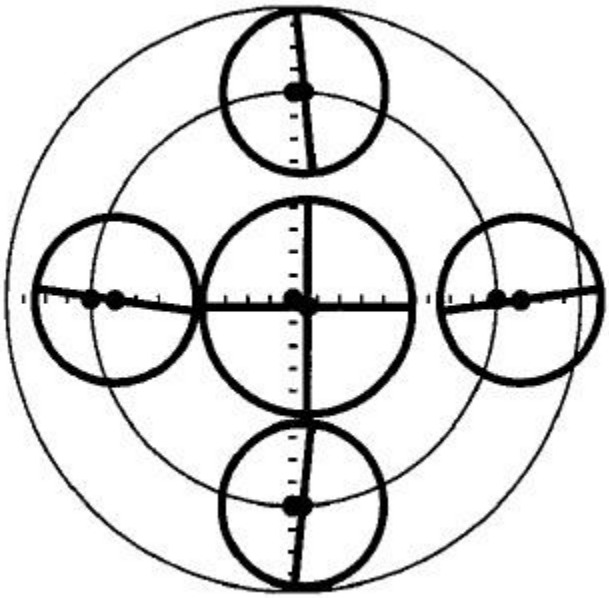

Figure 5.2: Translational Mode (R. G. Parker and J. Lin)

Table 5.3: Translational Mode Natural Frequencies

Multiplicity	2					
Frequency No.	2,3	4,5	8,9	11,12	16,17	19,20
Frequency (Hz)	727.27	1091.2	1892.8	2342.5	7189.9	10438

Table 5.4: Translational Mode Shapes (Matlab)

Frequency No.	2	3	4	5	8	9	11	12	16	17	19	20
Carrier												
X Disp	0.8354	-0.0986	-0.1764	-0.1764	0.0371	-0.2193	0.4131	0.0305	-0.0005	0.0214	0.0024	-0.0000
Y Disp	-0.0660	0.8335	-0.2596	-0.2596	-0.1924	-0.0000	-0.0000	-0.4193	-0.0216	0.0000	-0.0000	-0.0024
Rotational Disp	0.0000	0.0000	-0.0000	0.0000	-0.0000	-0.0000	-0.0000	0.0000	0.0000	-0.0000	0.0000	-0.0000
Ring												
X Disp	0.6305	-0.4631	-0.3981	-0.3981	0.1202	0.2586	-0.1431	-0.0172	0.0339	0.5539	-0.0124	-0.0181
Y Disp	0.3459	0.5516	1.0000	1.0000	0.2584	-0.1869	-0.0066	0.1447	-0.5591	0.0454	-0.0182	0.0126
Rotational Disp	0.0000	-0.0000	-0.0000	0.0000	-0.0000	-0.0000	-0.0000	0.0000	0.0000	0.0000	-0.0000	-0.0000
Sun												
X Disp	0.2573	0.1856	-0.5535	-0.5535	1.0000	-0.7265	-1.0000	-0.2779	-0.3063	0.3006	1.0000	0.1050
Y Disp	-0.2402	0.2998	-0.6103	-0.6103	-0.4681	-1.0000	-0.2012	1.0000	-0.2966	-0.2975	0.1123	-1.0000
Rotational Disp	-0.0000	-0.0000	-0.0000	-0.0000	-0.0000	-0.0000	-0.0000	0.0000	0.0000	0.0000	0.0000	-0.0000
Planet 1												
Radial Disp	1.0000	-0.1064	-0.0973	-0.0973	-0.7748	0.3676	-0.8939	0.2553	-0.3620	-0.1327	-0.0726	0.1210
Tangential Disp	-0.0367	0.6112	0.1180	0.1180	0.0727	-0.8124	-0.3165	0.4873	1.0000	0.3621	-0.1206	0.2014
Rotational Disp	0.5044	0.1296	0.9159	0.9159	-0.2467	0.6787	-0.0527	-0.2548	0.8712	0.3152	0.1818	-0.3034
Planet 2												
Radial Disp	-0.0908	1.0000	-0.4357	-0.4357	0.1851	0.8124	0.3165	0.9305	0.1415	-0.3621	0.1206	0.0716
Tangential Disp	-0.6150	0.0842	0.1186	0.1186	-0.7251	0.0737	0.5032	0.3583	-0.3863	1.0000	0.2007	0.1190
Rotational Disp	-0.2324	0.5409	-0.3430	-0.3430	0.5699	0.1504	-0.2473	0.0352	-0.3363	0.8712	-0.3023	-0.1794
Planet 3												
Radial Disp	-1.0000	0.1064	0.0973	0.0973	0.7748	-0.3676	0.8939	-0.2553	0.3620	0.1327	0.0726	-0.1210
Tangential Disp	0.0367	-0.6112	-0.1180	-0.1180	-0.0727	0.8124	0.3165	-0.4873	-1.0000	-0.3621	0.1206	-0.2014
Rotational Disp	-0.5044	-0.1296	-0.9159	-0.9159	0.2467	-0.6787	0.0527	0.2548	-0.8712	-0.3152	-0.1818	0.3034
Planet 4												
Radial Disp	0.0908	-1.0000	0.4357	0.4357	-0.1851	-0.8124	-0.3165	-0.9305	-0.1415	0.3621	-0.1206	-0.0716
Tangential Disp	0.6150	-0.0842	-0.1186	-0.1186	0.7251	-0.0737	-0.5032	-0.3583	0.3863	-1.0000	-0.2007	-0.1190
Rotational Disp	0.2324	-0.5409	0.3430	0.3430	-0.5699	-0.1504	0.2473	-0.0352	0.3863	-0.8712	0.3023	0.1794

iii. Planet modes: These modes have multiplicity m=1 for the given system. There is no displacement of sun gear, carrier as well as a ring gear. While planet motion takes place. Here, radial mode includes the radial displacement of the planets as well as their rotational displacement. While, tangential mode has only tangential displacements of the planets. While the rotational planet mode contains a little radial planet displacement as well.

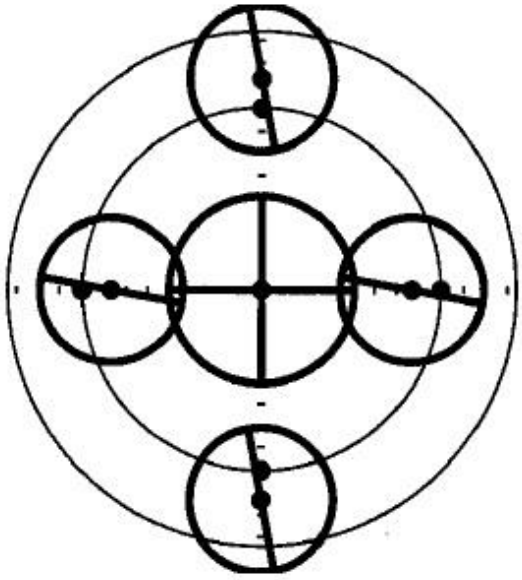

Figure 5.3: Radial Planet Mode

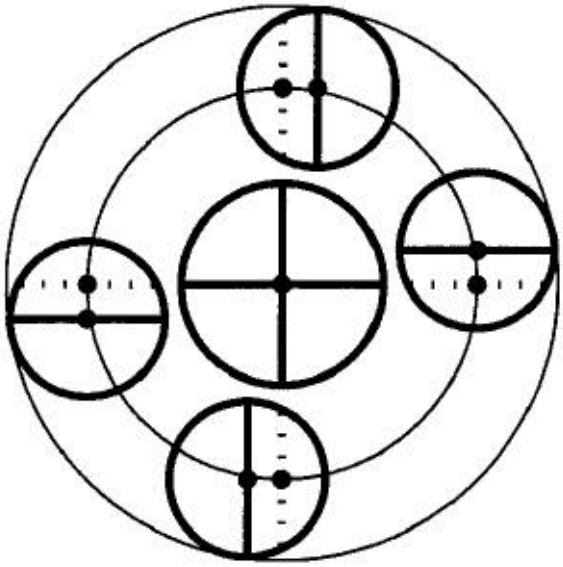

Figure 5.4: Translational Planet Mode

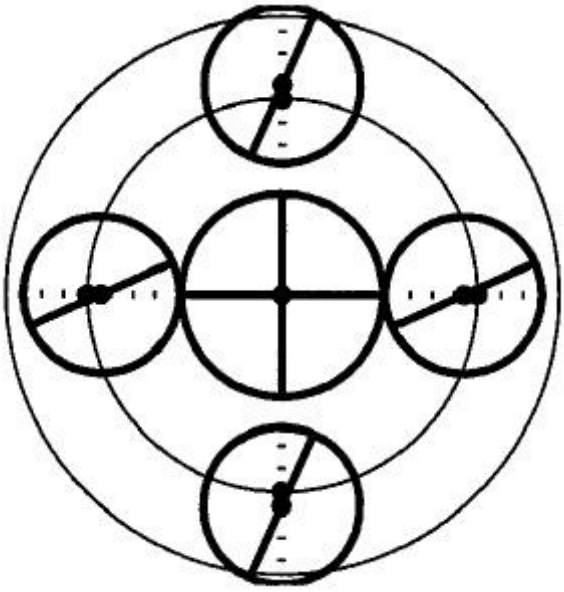

Figure 5.5: Rotational Planet Mode

Table 5.5: Planet Mode Natural Frequencies

Multiplicity	1		
Frequency No.	7	14	15
Frequency (Hz)	1808.28	5963.8	6981.7

Table 5.6: Planet Mode Shapes (Matlab)

Frequency No.	7	14	15
Carrier			
X Disp	-0.0000	-0.0000	-0.0000
Y Disp	-0.0000	-0.0000	-0.0000
Rotational Disp	-0.0000	-0.0000	-0.0000
Ring			
X Disp	-0.0000	-0.0000	-0.0000
Y Disp	-0.0000	-0.0000	0.0000
Rotational Disp	-0.0000	-0.0000	-0.0000
Sun			
X Disp	-0.0000	-0.0000	-0.0000
Y Disp	-0.0000	-0.0000	-0.0000
Rotational Disp	-0.0000	-0.0000	-0.0000
Planet 1			
Radial Disp	-1.0000	0.0000	-0.4176
Tangential Disp	-0.0000	1.0000	-0.0000
Rotational Disp	-0.4519	0.0000	1.0000
Planet 2			
Radial Disp	1.0000	0.0000	0.4176
Tangential Disp	-0.0000	-1.0000	-0.0000
Rotational Disp	0.4519	0.0000	-1.0000
Planet 3			
Radial Disp	-1.0000	0.0000	-0.4176
Tangential Disp	-0.0000	1.0000	-0.0000
Rotational Disp	-0.4519	0.0000	1.0000
Planet 4			
Radial Disp	1.0000	0.0000	0.4176
Tangential Disp	-0.0000	-1.0000	-0.0000
Rotational Disp	0.4519	0.0000	-1.0000

5.2 Sensitivity of Natural Frequency

Natural frequencies of the epicyclic gear can be affected by many factors. Here, the natural frequency can be plotted against many factors like the meshing stiffness, inertias and masses of the components.

It was found that by plotting the natural frequencies against the inertia of the sun gear, only the rotational frequencies produced a curve. While lower frequencies showed almost no change, higher frequencies have a tendency of variation against the changing value.

These analyses are very important, since they can show us the change in the natural frequencies and hence the behavior of the entire system.

Various design guidelines can be summarized from these sensitivity curves and can be used to predict the effect of various system parameters on planetary gear free vibrations.

5.2.1 Sensitivity due to Change in the Sun Gear Mass

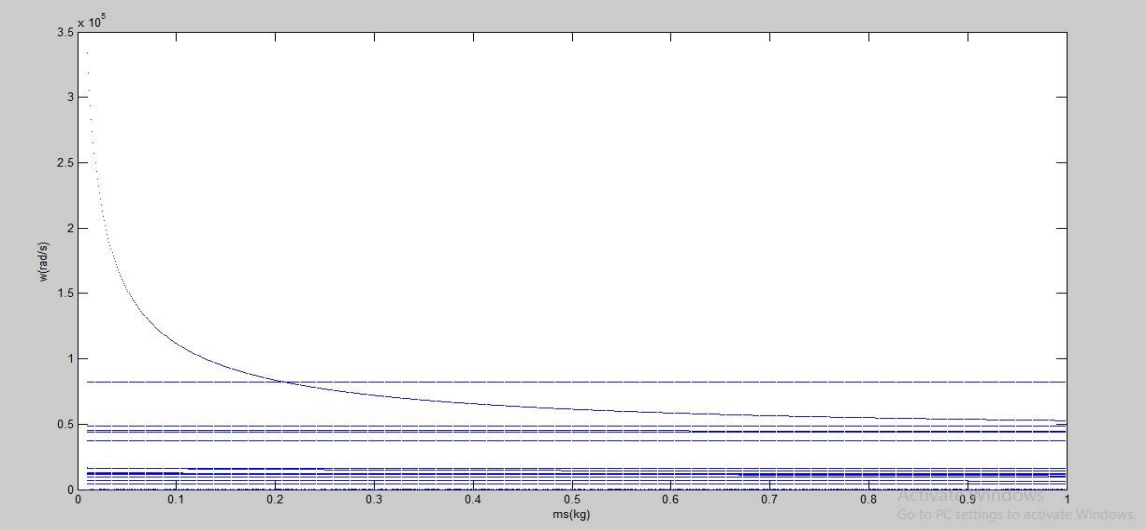

Figure 5.6: ω (rad/s) vs. ms (kg)

5.2.2 Sensitivity due to Change in the Ring Gear Mass

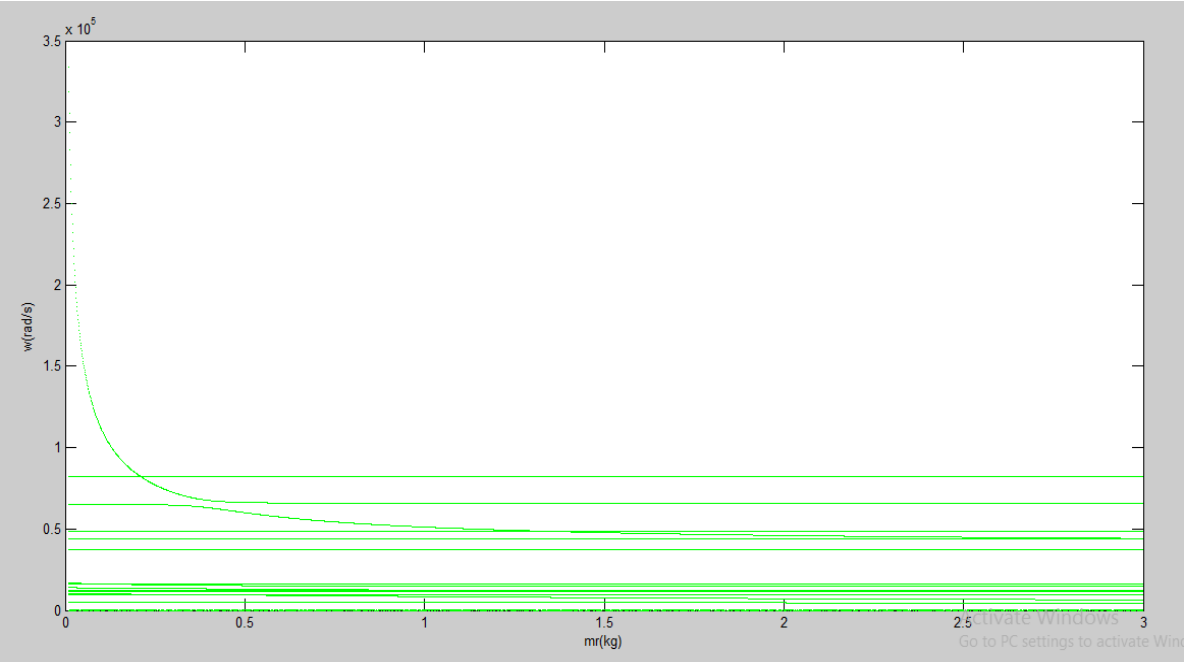

Figure 5.7: ω (rad/s) vs. mr (kg)

5.2.3 Sensitivity due to Change in the Planet Gear Mass

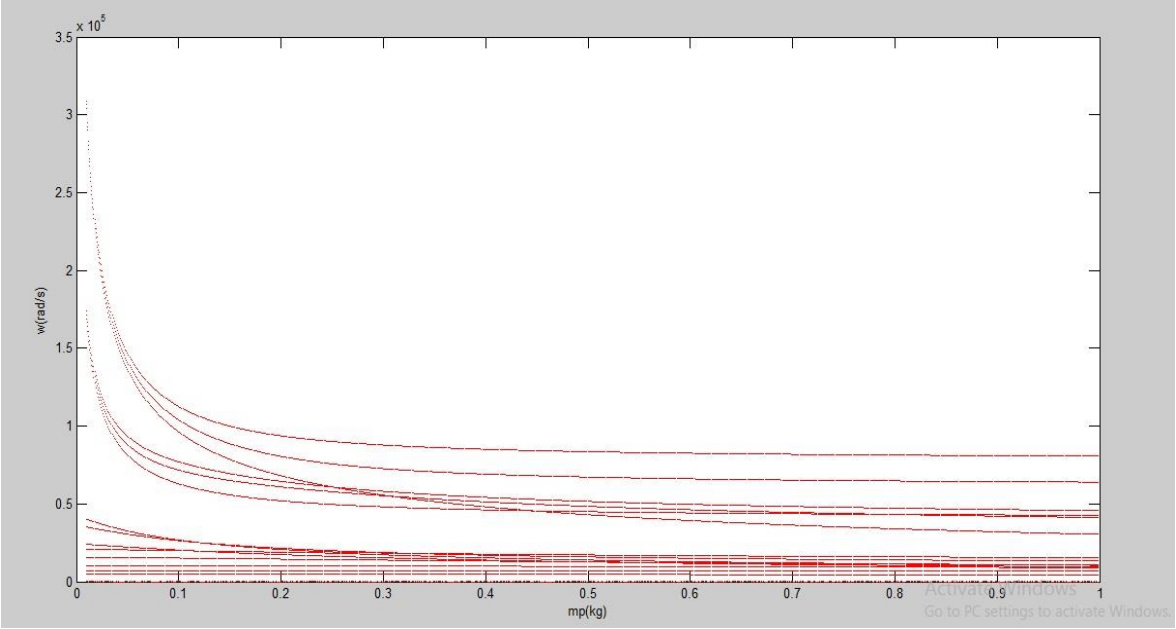

Figure 5.8: ω (rad/s) vs. mp (kg)

If we compare these results, we can observe that the variation in the planet gear mass affects the system vibration behavior most. As we get a clear idea about the effects of these parameters on the vibration of the epicyclic gears, this analysis is considered as an important one.

6 Conclusions and Recommendations

This research presented a methodology to calculate the meshing stiffness matrices for each meshing pair in the epicyclic gear set.

6.1 Conclusions

Some primary conclusions obtained from the research are given:

1. The obtained 6-DOF mesh stiffness matrix was used for coupling two node of the finite element analysis. This matrix can use both linear and non-linear mesh stiffness coefficient values into model.
2. This model is able to provide the contribution of all DOFs of the spur gear pair to a global coordinates system.
3. Meshing stiffness of the each gear pair depends on the number of meshing gear teeth in contact at a time. When the one pair of teeth is in contact at that time, the mesh stiffness of each gear pair decreases but as number of pairs in contact increase, the mesh stiffness value of gear pair increases.
4. Average value of the gear mesh stiffness is largely depends upon materials parameter of meshing gears.
5. The primary terms in the meshing stiffness matrix for each planet remain the same. Few terms like orientation angle and other dependent terms get changed.
6. Basically, the meshing $[k_{ij}]$ and $[k_{ji}]$ matrices of each gear pair are transpose of each other.

6.2 Limitation

Some limitations of this research were:

1. This model did not include the effect of the sliding action or friction and all the forces were assumed to operate at the pitch point along the LOA.
2. Proposed methodology was used to calculate the meshing stiffness of the meshing spur epicyclic gear pairs. It did not include load sharing factor amongst planets, tooth transmission errors and meshing teeth were assumed to be in contact all the time.

6.3 Recommendations

1. The effect of the sliding action and hence the friction can be used in the model.
2. The effect of non-linear mesh stiffness on the dynamic response of the meshing gear pairs in the epicyclic geared systems can be studied in detailed.
3. Inclusion of the backlash and transmission error would give more robust mathematical model.
4. Methodology can be extended to find out the meshing frequencies of the helical epicyclic gears.

References

[1]. Agashe V., “Computational Analysis of the Dynamic Response of a Planetary Gear System”, Master Thesis, Ohio State University.

[2]. Ahmed Hammami, Alfonso Fernandez Del Rincon, Fernando Viadero Rueda, “Modal Analysis of Back-To-Back Planetary Gear: Experiments and Correlation against Lumped-Parameter Model”, Journal of Theoretical and Applied Mechanics, 53, 1, p. 125-138.

[3]. A. Kahraman, “Dynamic Analysis of Geared Rotors by Finite Elements”, Mech. Mach., vol. 114, no. 3, p. 1151-1165, 1994.

[4]. A. Kahraman, “Planetary Gear Dynamics”, ASME, vol. 116, p. 713, 1994

[5]. Botman, M., "Epicyclic Gear Vibration", Journal of Engineering for Industry, vol. 96, p. 811-815, 1996.

[6]. Chun Hung Lee, “Non-Linear Contact Analysis of Meshing Gears”, Thesis, California Plotechnic State Institute, 2009.

[7]. David Blake Stringer, “Geared Rotor Dynamic Methodologies for Advancing Prognostic Modeling Capabilities in Rotary-Wing Transmission Systems”, Doctorate Dissertation, University of Virginia, 2008.

[8]. D. B. Stringer, P. N. Sheth and P. E. Allaire, “Modal Reduction of Geared Rotor System with General Damping and Gyroscopic Effects”, Journal of Vibration and Control, vol. 17, no. 7, pp. 975-987, 2010.

[9]. Kahraman, A. and Blankenship, “Planet Mesh Phasing in Epicyclic Gear Set”, Proc. of International Gearing Conference, Newcastle, UK, 99-104, 1994.

[10]. J. Lin and R. G. Parker, “Analytical Characterization of the Unique Properties of Planetary Gear Free Vibration”, Journal of Vibration and Acoustics, Vol. 121, P. 321, 1999.

[11]. J. Lin and R. G. Parker, “Sensitivity of Planetary Gear Natural Frequencies and Vibration Modes to Model Parameters”, Journal of Sound and Vibration, Vol. 228 (1), P. 109-128, 1999.

[12]. Jianming Wang and Liming Dai, “Survey of dynamics of planetary gear trains”, Int. J. Materials and Structural Integrity, vol. 1, no. 4, 2008.

[13]. S. Wadkar and S. Kajale, “Theoretical Evaluation of Effect of Gear Parameters on Mesh Stiffness Variations”, in Proceeding of the 14th international conference on mechanical engineering in knowledge edge, Delhi, 2005, pp. 148-153.

[14]. Tale Geramitcioski and Ljupco Trajcevski, “Theoretical Improvement of the Planetary Gear Dynamic Model”, International Design Conference, 2002.

Appendix A: Finite Element Matrix Equations

The given equations present the sub-matrices in the equation 4.58. All of these matrices are derived from the formulated equations.

A.1 3-DOF Meshing Matrices

The meshing sub-matrices are given as:

$$[Kc_1]^z = kp_z \begin{bmatrix} 1 & 0 & -\sin\varphi_z \\ 0 & 1 & \cos\varphi_z \\ \sin\varphi_z & \cos\varphi_z & 1 \end{bmatrix} \quad (A.1)$$

$$[Kc_2]^z = kp_z \begin{bmatrix} -\cos\varphi_z & \sin\varphi_z & 0 \\ -\sin\varphi_z & -\cos\varphi_z & 0 \\ 0 & -1 & 0 \end{bmatrix} \quad (A.2)$$

$$[Kc_3]^z = kp_z \begin{bmatrix} -\cos\varphi_z & -\sin\varphi_z & 0 \\ \sin\varphi_z & -\cos\varphi_z & -1 \\ 0 & 0 & 0 \end{bmatrix} \quad (A.3)$$

Here, $[Kpp]^z = [Kc_4]^z + [Kr_4]^z + [Ks_4]^z$ (A.4)

$$[Kc_4]^z = kp_z \begin{bmatrix} 1 & 0 & 0 \\ 0 & 1 & 0 \\ 0 & 0 & 0 \end{bmatrix} \quad (A.5)$$

$$[Kr_1]^z = kr_z \begin{bmatrix} \sin 2\varphi r_z & -\cos\varphi r_z \sin\varphi r_z & -\sin\varphi r_z \\ -\cos\varphi r_z \sin\varphi r_z & \cos 2\varphi r_z & \cos\varphi r_z \\ -\sin\varphi r_z & \cos\varphi r_z & 1 \end{bmatrix} \quad (A.6)$$

$$[Kr_2]^z = kr_z \begin{bmatrix} -\sin\varphi r_z \sin\alpha_r & \sin\varphi r_z \cos\alpha_r & \sin\varphi r_z \\ \cos\varphi r_z \sin\alpha_r & -\cos\varphi r_z \cos\alpha_r & -\cos\varphi r_z \\ \sin\alpha_r & -\cos\alpha_r & -1 \end{bmatrix} \quad (A.7)$$

$$[Kr_3]^z = kr_z \begin{bmatrix} -\sin\varphi r_z \sin\alpha_r & \cos\varphi r_z \sin\alpha_r & \sin\alpha_r \\ \sin\varphi r_z \cos\alpha_r & -\cos\varphi r_z \cos\alpha_r & -\cos\alpha_r \\ \sin\varphi r_z & -\cos\varphi r_z & -1 \end{bmatrix} \quad (A.8)$$

$$[Kr_4]^z = kr_z \begin{bmatrix} \sin 2\alpha_r & -\cos\alpha_r \sin\alpha_r & -\sin\alpha_r \\ -\cos\alpha_r \sin\alpha_r & \cos 2\alpha_r & \cos\alpha_r \\ -\sin\alpha_r & \cos\alpha_r & 1 \end{bmatrix} \quad \text{(A.9)}$$

$$[Ks_1]^z = ks_z \begin{bmatrix} \sin 2\varphi s_z & -\cos\varphi s_z \sin\varphi s_z & -\sin\varphi s_z \\ -\cos\varphi s_z \sin\varphi s_z & \cos 2\varphi s_z & \cos\varphi s_z \\ -\sin\varphi s_z & \cos\varphi s_z & 1 \end{bmatrix} \quad \text{(A.10)}$$

$$[Ks_2]^z = ks_z \begin{bmatrix} \sin\varphi s_z \sin\alpha_s & \sin\varphi s_z \cos\alpha_s & -\sin\varphi s_z \\ -\cos\varphi s_z \sin\alpha_s & -\cos\varphi s_z \cos\alpha_s & \cos\varphi s_z \\ -\sin\alpha_s & -\cos\alpha_s & 1 \end{bmatrix} \quad \text{(A.11)}$$

$$[Ks_3]^z = ks_z \begin{bmatrix} \sin\varphi s_z \sin\alpha_s & -\cos\varphi s_z \sin\alpha_s & -\sin\alpha_s \\ \sin\varphi s_z \cos\alpha_s & -\cos\varphi s_z \cos\alpha_s & -\cos\alpha_s \\ -\sin\varphi s_z & \cos\varphi s_z & 1 \end{bmatrix} \quad \text{(A.12)}$$

$$[Ks_4]^z = ks_z \begin{bmatrix} \sin 2\alpha_s & \cos\alpha_s \sin\alpha_s & -\sin\alpha_s \\ \cos\alpha_s \sin\alpha_s & \cos 2\alpha_s & -\cos\alpha_s \\ -\sin\alpha_s & -\cos\alpha_s & 1 \end{bmatrix} \quad \text{(A.13)}$$